Republic of Iraq
Ministry of Higher Education & Scientific Research
University of Babylon
College of Education for Pure Sciences
Department of Physics

An Analytical Study of Quasi-Elastic Scattering for some Systems Using the Woods-Saxon Potential

A Thesis

Submitted to the Council of the College of Education for Pure Sciences of University of Babylon in Partial Fulfillment of the Requirements for the Degree of Master in Education / Physics

By

Nagham Hassan Hayef Ali

B. Sc. in Physics

(University of Baghdad, 2003)

Supervised by

Prof. Khalid Salih Jassim (Ph.D.)

2021 A.D. **1443 A.H.**

بِسْمِ اللهِ الرَّحْمَٰنِ الرَّحِيمِ

أَمَّنْ هُوَ قَانِتٌ آنَاءَ اللَّيْلِ سَاجِدًا وَقَائِمًا
يَحْذَرُ الْآخِرَةَ وَيَرْجُو رَحْمَةَ رَبِّهِ ۗ قُلْ هَلْ
يَسْتَوِي الَّذِينَ يَعْلَمُونَ وَالَّذِينَ لَا
يَعْلَمُونَ ۗ إِنَّمَا يَتَذَكَّرُ أُولُو الْأَلْبَابِ ۞

صَدَقَ اللهُ العَلِيُّ العَظِيمُ

(سورة الزمر الآية 9)

Dedication

I dedicate this study and all the effort that went into it to my family, especially my dear mother, and to my children who supported and encouraged me, as I dedicate it to all the martyrs of Iraq, especially my beloved father, the martyr (Hassan Hayef Ali) and my husband, the martyr (Ahmed Mansour Hussein) mercy and eternity for their pure souls.

Acknowledgements

First and foremost, I thank Allah who gave me strength, inspiration and prudence to bring this thesis to a close. I would like thank my supervisor , **Prof. Khalid Salih Jassim (Ph.D.)**, Dean of the College of Education for Pure Sciences, University of Babylon for his effort, good directives and suggestions made this work successful. May Allah keeps him healthey and always helps him to serve science. My thanks and appreciation to my family for their unlimited support .My thanks and gratitude to all faculty members in the Department of Physics for their unlimited support. I would also like to thank my colleagues, especially those who graduated with their master›s in Physics from the previous cohort, for their generous support and assistance.

Supervisor Certificate

This is to certify that I have read this thesis entitled **"An Analytical Study of Quasi-Elastic Scattering for some Systems Using the Woods-Saxon Potential"** by **"Nagham Hassan Hayef Ali"** has been prepared under my supervision in University of Babylon / College of Education for Pure Sciences as a partial requirement for the Degree of Master in Education / Physics.

Signature :

Name : Dr.Khalid S.Jassim

Title: Professor

Date: / / 2021

Head of Physics Department

In view of the available recommendation, I forward this thesis for debate by the examining committee.

Signature:

Name: Dr. Khalid H. Abbas

Title: Professor

Date: / / 2021

Certification of Scientific Expert

I certify that I have read the scientific contents of this thesis **"An Analytical Study of Quasi-Elastic Scattering for some Systems Using the Woods-Saxon Potential"** and I have approved this thesis is qualified for debate.

Signature:

Name: Dr. Ali Abid Abojassim

Title: Professor

Date: / /2021

Certification of Linguistic Expert

I certify that I have read this thesis entitled **"An Analytical Study of Quasi-Elastic Scattering for some Systems Using the Woods-Saxon Potential"** and corrected it is grammatical mistakes; therefore ,it has qualified for debate.

Signature:

Name:Dr.Mais F .Hasan

Title: prfessor

Date: / / 2021

Certification of Scientific Expert

I certify that I have read the scientific contents of this thesis **"An Analytical Study of Quasi-Elastic Scattering forsome Systems Using the Woods-Saxon Potential"** and I have approved this thesis is qualified for debate.

Signature:

Name: Dr. Rajaa K.Mohammad

Title: Assistant Professor

Date: / /2021

Examining Committee Certification

We certify that we have read the thesis entitled **"An Analytical Study of Quasi-Elastic Scattering for some Systems Using the Woods-Saxon Potential"** by **"Nagham Hassan Hayef Ali"** and as a committee examined the student in its contents and, according to our opinion, it is accepted as a thesis for the Degree of Master in Education / Physics .

Signature:

Name: Dr. Fouad A. Majeed

Title: Professor

Date: / / 2021

Chairman

Signature:

Name: Dr. Mohanad H. Oleiwi

Title: Ass.Prof.

Date: / / 2021

Member

Signature:

Name: Dr.Samah O.Hassoon

Title: Ass.Prof.

Date: / / 2021

Member

Signature:

Name: Dr. Khalid S. Jassim

Title: Professor

Date: / / 2021

Member / Advisor

I hereby certify the decision of the examining committee.

Signature:

Name: Dr. Bahaa Hussien Salih Rabee

Title: Professor

Address: Dean of the College of Education for Pure Sciences

Date: / / 2021

Abstract

This study, a systematic study was performed on the quasi-elastic scattering, through which the effect surface-level diffusion parameters of the nuclear potential on the cross-section calculations in the quasi-elastic scattering to that same cross-section of Rutherford was carried out and was taken in all coupling orders single channel (SC) and coupled channels (CC) and this scattering occurs between two nuclei and more than one system. The interacting nucleus systems for the present study are: $^{6}Li + ^{64}Zn$, $^{23}Na + ^{90}Zr$, $^{11}C + ^{208}Pb$, $^{16}O + ^{208}Pb$, $^{16}O + ^{63}Cu$. The potential describing the interactions between the nuclei consisting of a Coulomb and a Nuclear potential, nuclear potential has been described using the Woods - Saxon potential (WS).

Calculations of the single channel (SC) and coupled channels (CC) defining relative movement and inherent colliding nuclei movements. where carried out with the study their effect on the calculations of the cross-section ratio of quasi-elastic scattering to the cross-section of Rutherford scattering as the coupled channels (CC). Best fit value of diffusion parameters compared to experimental data. The program used in this study is CQEL, which was developed by the Japanese researcher Hagino and his colleagues. We used the chi-square χ^2 methods to select the most suitable match for the value of the diffusion parameter with the experimental data best diffusion parameter obtained from coupling channel calculations for an inert projectile and excited target for systems $^{6}Li + ^{64}Zn$, $^{23}Na + ^{90}Zr$, (^{11}C and ^{16}O) + ^{208}Pb, and an inert target and excited projectile of the $^{16}O + ^{63}Cu$ system. As the obtained diffusion parameters compared to the standard value of 0.63 fm they are fully compatible with all the above systems.

Contents

List of Abbreviations and Symbols

Abb. Symbol	Abb. Definition
a	The surface diffuseness parameter.
A_{lm}	The expansion coefficient of expanding the wave function $\psi(\vec{r})$, represents the capacity of the wave function.
$a_{\lambda\mu}$	The phonon annihilation operator
$a^{\dagger}_{\lambda\mu}$	The phonon creation operator
α_o	The amplitude of the zero-point motion
$\alpha_{\lambda\mu}$	The coordinate of the surface vibration.
A_P	The mass number of the projectile nucleus.
A_T	The mass number of the target nucleus.
β_λ	The deformation parameter
B(Eλ) ↑	The electromagnetic transition probability.
^{11}C	The isotope of Carbon.
CC	The coupled-channels.
^{63}Cu	The stable isotopes of Copper
E	The eigen value of the Hamiltonian operator.
e	Electron charge.
η	The Summerfield parameter.
f_c	The Coulomb scattering amplitude.
$f(\theta)$	The scattering amplitude.
$f_\lambda^C(r)$	The Coulomb coupling form factor.
$f_\lambda(r)$	Coupling form factor.
H	The Hamiltonian operator.
$H_0(\xi)$	For intrinsic motion, the Hamiltonian.
$H_l^{(-)}(kr)$	The incoming Coulomb wave.
$H_l^{(+)}(kr)$	The outgoing Coulomb wave.
I	The intrinsic angular momenta.
J	The total angular momentum.
$\vec{k}$	The wave number vector of the incoming wave.
$k_{nlJ}(r)$	The local wave number .
L	The orbital angular momentum.
^{6}Li	The stable isotope of Lithium.
λ_μ , $\|\mu\rangle$	The operator's eigenvalue and eigenvector $\hat{O}_\lambda$.
λ_P	The vibrations in the projectile are multi-polar..
λ_T	Vibrations in the target have several polarities.
^{23}Na	The stable isotope of Sodium.
^{16}O	The stable isotopes of Oxygen.

$\hat{O}_{\lambda}$	The dynamical operator.
$Q_{\hat{\lambda}\hat{\mu}}$	The electric multipole operator.
$\hat{O}_{\lambda_P}$	The projectile excitation operators.
$\hat{O}_{\lambda_T}$	The excitation operators for target .
^{208}Pb	The stable isotope of Lead.
$P_{lIli}^{J}(E)$	The penetrability during the Coulomb barrier.
$\varphi_{nIm_I}(\xi)$	The wave function for the intrinsic motion.
ϕ_d, θ_d, χ_d	The Euler angles.
$\psi(\vec{r})$	The wave function of the incoming plane wave.
$\psi(r,\theta)$	The wave function of the sum of incoming plane wave and The outgoing spherical wave.
R_o	Radius parameter of the system.
r_0	The radius parameter.
r	Center- of-mass distance between projectile and target nuclei.
R_B	The position of the Coulomb barrier.
R_C	The Coulomb radius.
R_T	Equivalent sharp radius.
$R_T(\theta,\phi)$	The radius in vibrating target nucleus.
ρ_T	The charge density of the target nucleus
SC	The single-channel.
S_l	The complex quantity nuclear S-matrix.
σ_{el}	The total elastic cross section.
σ_R	The Rutherford cross section.
$\mathrm{T}_{\lambda\mu}(\xi)$	The spherical tensors.
$\mathcal{T}_{nlI}^{J}$	The transmission coefficients.
θ	The angle between $\vec{r}$ and $\vec{k}$.
$U_l(r)$	The diagonal part of the wave function $\psi(\vec{r})$.
V_0	The potential depth.
$V_c(r)$	The Coulomb potential.
$V_{coup}(\vec{r}.\xi)$	The coupling Hamiltonian of the system.
$V_C^{coup(vib)}(\vec{r},\alpha_{\lambda\mu})$	The Coulomb vibrational coupling potential.
$V_{eff}(l,r)$	The effective potential
$V_{mn}^{N}(r)$	The nuclear coupling matrix elements.
$V_N(r)$	The Nuclear potential.
$V_N^{coup(vib)}(r,\hat{O}_{\lambda})$	The nuclear vibrational coupling potential.
$V_N^{coup(rot)}(r,\hat{O}_{\lambda})$	The nuclear rotational coupling potential
$V_{nlI;\acute{n}\,l'\acute{I}}^{J}(r)$	The coupling matrix elements.

WS	The Woods-Saxon.
ξ	Internal degree of freedom.
$\xi_{\alpha(\gamma)}$ and $\|\alpha(\gamma)\rangle$	For the operators $\hat{O}_{P(T)}$, the eigenvalues and eigenvectors
$Y_{lm}(\vec{r})$	The angular part of the wave function $\psi(\vec{r})$.
^{64}Zn	The stable isotopes of Zinc .
Z_P	Projectile Atomic number.
^{90}Zr	The stable isotope of Zirconium.

List of Tables

List of Figures

Chapter One

Introduction and Literature Survey

Chapter One

Introduction and Literature Survey

1.1 Introduction

Fusion and quasi-elastic scattering are two systems that work together. As a result, these reactions have the same potential and knowledge about the reaction mechanism. As a result, nuclear potential can also be investigated via quasi elastic scattering..

Looking at the fusion barrier distribution using the excitation function of quasi-elastic scattering near the barrier energies is equal to looking at the fusion barrier distribution using the excitation function of quasi-elastic scattering near the barrier energies.

The nuclear potential has been investigated using large-angle quasi-elastic scattering [1-3]. The coupling channel (CC) model is an excellent tool for re-producing experimental data for several processes at the same time, such as elastic and inelastic scattering, particle transfers, and fusion, in a single framework [4-7] . In their approach, Washiyama et al. [2] , conducted a systematic study of the surface diffuseness parameter ,their results show that for spherical reaction systems, to match the quasi-elastic scattering data, a surface diffuseness parameter of roughly 0.6 fm is required, whereas a bigger diffuseness value of (0.8–1.1) fm is preferable for deformed reaction systems. In measurements of elastic and inelastic scattering, both of which are primarily susceptible to the surface area of the nuclear potential, the accepted value of the surface diffuseness parameter, 0.63 fm, has been employed [2].The nuclear potential can be studied using quasi-elastic scattering or fusion experimental results [8,9].When elastic scattering, inelastic scattering, and the transition reaction are put together, the result is quasi-elastic scattering. [2,10-13]. It closely resembles the fusion reaction [10,12], this is characterized as a reaction

in which two distinct nuclei combine forming a compound system [7, 14] . Both fusion and quasi-elastic scattering are called comprehensive operations and are mutually beneficial. As a result, all interactions are vulnerable to channel binding impacts (due to mutual inelastic excitements of colliding nuclei) at energies near the Coulomb barrier [11,15] . Both are affected by the same potential and have a similar knowledge of how things work together [1, 16,7].

Knowing the nuclear potential is very important to describe certain aspects of the interactions of heavy and medium ions in the form of a Woods-Saxon (WS), characterized by depth V_0 and radius r_0 , and the diffusion parameters *a* are adopted for the purpose of describing the nuclear potentials of elastic and inelastic scattering, which is sensitive to potential nuclear materials in the surface area [18,19].

A diffuseness parameter of 0.63 fm is generally appropriate for representing elastic and inelastic scattering data [18-23]. The combined Coulomb and Woods-Saxon nuclear potentials result in a separation interval barrier of 12 fm in Figure 1.1.

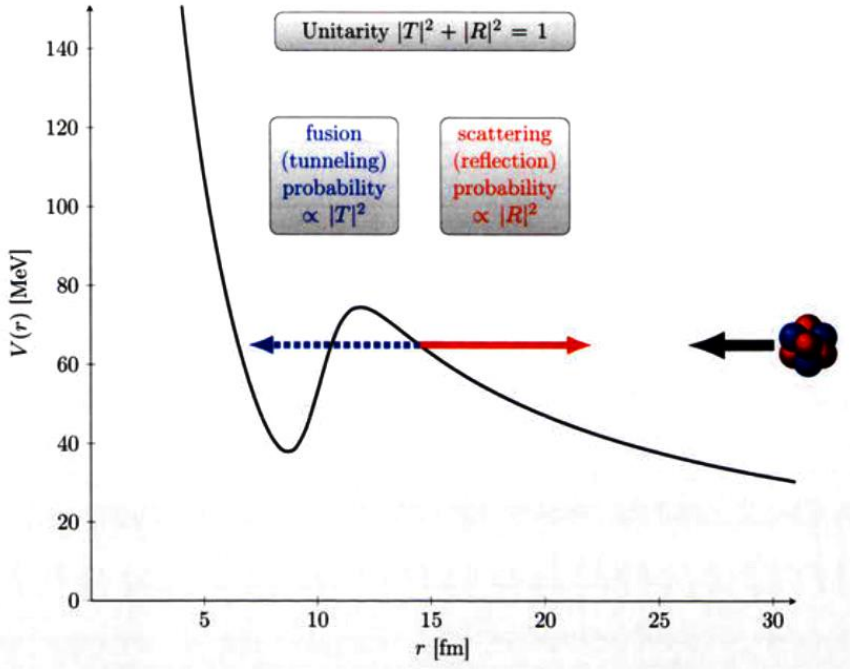

Figure 1.1 : The total inter-nuclear potential for ^{16}O colliding with ^{208}Pb [24].

Incident atoms with energy below the melting barrier are reflected (red arrow) or will funnel and pass through the barrier (blue arrow), resulting in melting. The amplitude squared of the coefficient of reflection R determines the quasi-elastic probability of scattering, while the amplitude squared of the coefficient of transmission T determines the probability of fusion [25]. The quantity of quasi-elastic scattering is calculated by adding the elastic scattering, the inelastic scattering, and the transition interaction with the result. In terms of fusion, it is thought to be a good match in order to quasi-elastic scattering, which is described as the fusion of two distinct nuclei to form a complex system. In a nutshell, quasi-elastic fusion and dispersion are two distinct mechanisms that work in tandem [9]. At deep sub-barrier energies, channel couplings may therefore be justified in omitting them from studies. This is only valid for spherical collision structures, according to Gasques et al. [3]. Many of the systems we've looked at so far are spherical. As a result, At deep sub-barrier energies, it is reasonable to ignore channel couplings. The ability to disregard channel couplings is one of the most important advantages of doing research at deep sub-barrier energy , simplifying calculations. As a result, computational instabilities in the equations should be avoided, lowering the precision of the analyses . Coupled-channels simulations for different heavy-ion systems have been conducted, taking into account certain coupling effects, and the results have been published. It was successfully conducted in experiments involving fusion reactions and quasi-elastic reverse angle scattering [1].

1.2 Literature Survey

There are many research studies close to the current study and some are to be mentioned here :

In (1995) , H. Timmers, et al. [26], have been calculated Quasi-elastic back-scattering stimulation functions of ^{16}O on ^{92}Zr, ^{144}Sm, ^{154}Sm, and ^{186}W targets . They compared the findings, also included are barrier distributions derived from fusion data and coupled-channel observations. They discovered that fusion is possible below the medium boundary energy using quasi-elastic scattering models.

In 1999, C. Morton et al. [27], showed that the fission excitation mechanism for the $^{16}O+^{208}Pb$ system was re-measured with improved precision, and CC measurements were used to explain the form of the fusion barrier distribution of the $^{16}O+^{208}Pb$ system, avoiding estimation to first-order coupling and constant-coupling, which are sometimes used in simpler analyses. This research looked at the excitation energy and phonon character of the single and double-phonon states of ^{208}Pb.

In (2000), S. Sastry and S. Santra [28], explained the coupled reaction channel (CRC) was used because these channels have a major impact on the fusion's excitation function. Elastic and quasi-elastic pathways, on the other hand, will unambiguously restore the structure and the reaction in a parallel analysis of the fusion. The fusion excitation functions for the ^{16}O + ^{208}Pb method, for example, are equipped with the same fusion barrier distributions for nuclei with different structures.

In (2002) ,T. J. Schuck *et al.* [29], had been evaluated Quasi-elastic scattering data back ward angles for the systems $^{34,32}S$ + ^{197}Au and $^{34,32}S$ + ^{208}Pb

for energies spanning the Coulomb barrier have been extracted from the data for the fusion reactions of $^{34,32}S$ with ^{197}Au.

In (2003), I. Gontchar *et al*. [30], shown that in order to balance the experimental results for ^{16}O + ^{208}Pb and ^{12}S+ ^{208}Pb structures, the Woods-Saxon (WS) potential diffusion parameters must be equal to 1fm for the over barrier energies and fusion cross-sections. These diffuseness parameter values were high when compared to elastic scattering values. The nucleus-nucleus potential was calculated using the double folding model, which was used to estimate fusion barrier energies and nuclear potential diffusion.

In (2006), K. Hagino *et al*. [2], discussed for a Woods-Saxon inter nuclear potential, it was inferred that a high value of the surface diffuseness parameter was used, is a successful fusion reaction comparable using quasi-elastic large-angle scattering to explore the possible ingredients that are missing from existing nuclear reaction models and to clarify the obvious inconsistency in the diffuseness parameter for fusion reactions.

In (2007), K. Hagino [31], showed that the surface diffuseness parameter of the nucleus-nucleus potential was calculated using quasi-elastic scattering of deep-sub barrier energies, and coupling channels for quasi-elastic barrier distribution were investigated for the ^{70}Zn +^{208}Pb reaction. The coupling-channel equations, which include multi-phonon excitations in the collisioning nuclei, demonstrate that the experimental excitation process for quasi-elastic reverse angle scattering and the barrier distribution for this reaction are reasonably well reproduced .

In (2009),K. Hagino [32], showed the lowest barrier in the barrier distribution is believed to be regulated by fusion cross sections deep-sub barrier energies, and the surface region of the inter nuclear potential is determined using quasi-elastic scattering site energy at a distance of sub-barrier, while an

inner component is calculated using the Semi classical formula. They used this method to study the reactions $^{16}O + ^{144}Sm$ and $^{16}O + ^{208}Pb$.

In (2010), I . Dutt and R. K. Puri [33], discussed the effect of surface diffuseness parameters, in addition to atomic surface diffusion, on the nearness potential and finishing of a mixture of heavy ions was investigated, with various surface diffuseness parameter variants being used. Such advanced criteria were thought to have a significant impact on the mixture obstacles.

In (2012), V. Scuderi *et al*. [34], were showed that at energies near the Coulomb limit, the elastic scattering and direct reactions for collisions caused by the three Beryllium isotopes $^{9,10,11}Be$ on a medium weight target of ^{64}Zn were investigated. In the Coulomb-nuclear interference peak angular area, the elastic-scattering angular distribution of the ^{11}Be halo nucleus deviated from the classical Fresnel type diffraction operation. They estimated that overall reaction cross-sections for the ^{11}Be collision are more than a factor of two larger than those calculated for the collisions caused by $^{9,10,11}Be$. They also discovered that transition and break-up mechanisms contribute significantly to the total reaction cross-section for ^{11}Be with inert objective and vibrational projectile are 0.44 fm, 0.67 fm, and 0.67 fm for all systems above, respectively, using the chi square form.

In (2013), S. Yusa *et al*. [35], were showed that is in a random matrix model, they described excitations that were explicitly taken into account in their calculations of the coupled channels. The non-collective excitations will reproduce the calculated smearing of the peak structure in the $^{20}Ne+^{90}Zr$ barrier distribution while not greatly altering the structure in the ^{92}Zr system. In ^{90}Zr, the difference is mostly due to the closed neutron shell.

In 2014, Khalid S. Jassim *et al*. [36], explored the nuclear potential for heavy ion systems using large-angle quasi-elastic scattering at sub-barrier

energies near the Coulomb barrier height, including ^{48}Ti, ^{54}Cr, and ^{64}Ni + ^{208}Pb systems. It is presumed that the nuclear potential is in WS form. He determined that the diffuseness parameter values most suited for researching systems were acquired through a coupled channel measurement.

F. A. Majeed *et al*. [37], (2014) for the systems ^{16}O+ ^{144,154}Sm, showed the distribution of the effect of the coupled channel on the calculation of total fusion reactions cross-sections and the fusion barrier were seen. The effect of the coupled channel on the measurement of the total fusion reactions cross-section . Single, octupole, and quadruple phonon excitations were taken in to consideration in the ^{144}Sm nucleus, while rotational deformation was included in the ^{154}Sm nucleus. He discovered that coupling of the octupole state within the ^{154}Sm target nucleus is very interesting, as it leads to an increase in total fusion cross section measurements and a strong fit to experimental data for fusion barrier distributions.

In 2015, K. Hagino and N. Rowley [38], discussed the ^{16}O+ ^{144,154}Sm, ^{58}Ni+ ^{58}Ni, and^{12}C +^{12}C systems. They examined how one can obtain the same expression with quasi-elastic cross-sections of scattering employing the so-called sum-of-differences (SOD) approach. The SOD barrier distribution, in contrast to the conventional quasi-elastic barrier distribution, has the benefit of being applicable to both non-symmetric and symmetric structures. It's also worth mentioning that the fusion barrier's distribution corresponds to a significantly larger range than that of quasi-elastic barriers..

In 2015, V. Kovalchuk [39], showed the nuclear diffraction model and the nucleus-nucleus scattering model in the high-energy approximation with a double folding potential for the intermediate energies of the incident particles were used to describe the cross-sections of quasi-elastic scattering of ^{6}He, ^{7}Be, and ^{8}B nuclei by ^{12}C nuclei. The calculations employed real nucleon density

distributions and took into consideration the Coulomb interaction and inelastic scattering with the excitation of the target's low-lying collective states.

In 2016, J. P. Fernández -García, *et al*. [40], studied the continuum discrete coupling approach, which was used to test the experimental distributions of elastic scattering angular distributions of collisions that included the weakly bound nuclei ^{6,7}Li and the halo nucleus ^{6}He on the same ^{64}Zn target at several energies around the Coulomb barrier . While the ^{6}He+^{64}Zn was compared with all continuum discrete results.

In 2018 ,T. Tanaka, *et al*. [42] .They were showed that exciatation functions for quasi elastic (QE) cross sections were measured for the reactions relevant to the synthesis of superheavy nuclei ,the ^{48}Ca +^{208}Pb ,^{50}Ti +^{208}Pb and ^{48}Ca+^{248}Cm systems .Owing to the excellent performance of the gas-filled type recoil ion separator GARIS and the focal plane detector system ,QE scattering events were effectively separated from deep –inelastic (DI) and precise barrier distributions were deduced for all of these systems .

In 2019, Q. J. Tarbool, *et al.* [43], showed that is the surface property of the inter-nucleus potential in heavy-ion reactions was investigated using large-angle quasi-elastic scattering at energies below the Coulomb barrier height for ^{6,7}Li + ^{64}Zn systems . The nuclear potential was calculated using the Wood Saxon (WS) calculation .For the nucleus ^{64}Zn, the result of rotational deformation was included, with ground state rotational banded up to the 4+ states, to elicit the diffuseness parameter of the nuclear potential as well as the potential depth, single-channel (SC) and coupled-channels (CC) calculations were performed using the (CQEL) software.

In (2020), A. J. Hassan, and K. S. Jassim [44], studied the effects of the surface diffuseness parameter on quasi-elastic scattering were investigated using

the Woods-Saxon (WS) nuclear potential systems $^{6}He+^{64}Zn$, $^{7}Li+^{64}Zn$, and $^{8}Li+^{90}Zr$.

1.3 The Aim of the Current Study

This research aims to achieve inter-nucleus potential surface diffuseness parameters in Woods-Saxon Potential for $^{6}Li + ^{64}Zn$, $^{23}Na + ^{90}Zr$, $^{11}C + ^{208}Pb$, $^{16}O + ^{208}Pb$, and $^{16}O + ^{63}Cu$ systems.

Chapter Two

Theoretical Background

2.1 Introduction

The detection of nuclear collisions generated by the halo and stable weakly bound nuclei, such as ^{6}Li and ^{7}Li, at energies around the Coulomb barrier has attracted a lot of interest. (see, for example, Ref. [45]). ^{6}Li nuclei have weakly bound cluster structures, i.e., $^{6}\text{Li} = \alpha + d$, with separation energies S_{α} = 1.47 MeV [46]. The coupling to the break-up channel will, have an effect in fact. The reaction dynamics and, as a result, strong effects on elastic scattering and fusion (e.g. [45, 47]). At near-barrier energies, the barrier diffusion approach has been proposed as an effective instrument for studying the effects of couplings to various reaction channel. [48,49]. The quasi-elastic scattering barrier distribution (D_{qel}) is defined as [29], $D_{qel}(E) = -\frac{d}{dE}\left[\frac{d\sigma_{qel}}{d\sigma_{Ruth.}}\right]$. At a constant backward angle, the ratio of quasi-elastic (QEL) scattering to Rutherford differential cross sections is $d\sigma_{qel}/d\sigma_{Ruth}$. QEL scattering is the total of elastic and inelastic scattering, as well as all other direct approaches [50].

2.2 Mathematical Background

The formalism is given a more rigorous mathematical context in the subsections that follow. The coupled-channels equations are deduced in a manner that closely resembles the notation Refs [24, 51] conventions .The aim of this section is to emphasize the model's simplicity and beauty, as well as to introduce the fundamental quantities required to understand the results of the quasi-elastic scattering calculations provided in this thesis.

There are two components of the nucleus-nucleus potential. They are the nuclear element $V_N(r)$, which can be well and reasonably defined by the WS form given by:[52]

$$V_N(r) = -\frac{V_0}{1+\exp\left[\frac{r-R_0}{a}\right]} \tag{2.1}$$

$$R_0 = r_0\left(A_T^{\frac{1}{3}} + A_P^{\frac{1}{3}}\right) \quad , \tag{2.2}$$

where R_0 is the system's radius parameter, V_0, a, and $r_0$are the parameters for potential depth, surface diffuseness, and radius, respectively.

The letter r represents the difference in center-of-mass between the target nucleus of mass number A_T and the projectile nucleus of mass number A_P. The diffuseness parameter expressed the property at the nuclear potential surface, where a_0 = 1 fm (represented by the dotted line in Figure 2.1) expands nuclear potential [53] . On the other hand, when no interaction occurs between two sphere nuclei with typical charge density distributions, the Coulomb component $V_C(\mathrm{r})$ is created given by [54]

$$V_C(\mathrm{r}) = \frac{Z_p Z_T \mathrm{e}^2}{\mathrm{r}} \qquad r > R_C \tag{2.3}$$

Where Z_P, Z_T, e, and r are the projectile's atomic number, the target's atomic number, the elementary charge, and the distance between colliding nuclei's centers (Gaussian units),respectively. The Coulomb potential is given as when the nuclei overlap [54].

$$V_C(r) = \frac{Z_p Z_T e^2}{2R_C}\left[3 - \left(\frac{r}{R_C}\right)^2\right] \qquad r \leq R_C \tag{2.4}$$

Where $R_C = r_C(A_T^{\frac{1}{3}} + A_P^{\frac{1}{3}})$, R_C is the radius of the target's and projectile's similar spheres. Elastic and inelastic scattering measurements are a popular technique for probing the inter-nuclear interaction potential, and optical model studies of elastic scattering cross sections within the optical model resulted in an average normal diffuseness value of $a_0 \sim 0.63$ fm of the nuclear potential [55].

Between the projectile and the target, a potential occurs as a function of the relative distance r between the nuclei's centers of mass. It is divided into two sections, as indicated by [55].

$$V(r) = V_N(r) + V_C(r) \tag{2.5}$$

The Schrödinger radial equation includes an effective potential, which is defined as follows [52].

$$V_{eff}(\ell, r) = V_N(r) + V_C(r) + \frac{\hbar^2 \ell(\ell+1)}{2\mu r^2} \tag{2.6}$$

Effective potential is the number of the nuclear, Coulomb, and centrifugal elements. The centrifugal compound vanishes between the two at angular momentum $\ell = 0$. The nucleus-nucleus relationship is $\ell = 0$ at zero angular momentum.

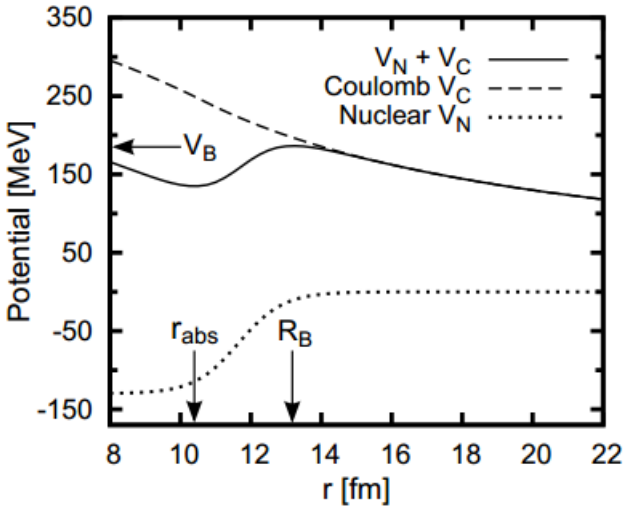

Figure 2.1: A typical nucleus-nucleus potential of a heavy-ion system at $l = 0$, [52].

The nuclear potential $V_N(r)$, the Coulomb potential $V_C(r)$, and other potentials. The entire nuclear and Coulomb potentials by dotted, dashed, and strong lines, respectively [52].

The nucleus-nucleus potential, V_B, which is placed at a distance R_B between the centers of colliding nuclei, produces the Coulomb barrier height [50] .

2.3 Formal Theory of Scattering

In this part, the fundamental equation for calculating elastic and fusion cross-sections is derived using a single-channel potential model. The Schrödinger equation for three-dimensional relative motion is as follows: [7]

$$\left[-\frac{\hbar^2}{2\mu}\nabla^2 + V(r) - E\right]\psi(\vec{r}) = 0, \qquad (2.7)$$

where $V(r)$ is the sum of nuclear and Coulomb potentials $V(r) = V_N(r) + V_C(r)$, μ the system's reduced mass, E is total energy, ∇^2 is Laplacian operator and $\hbar$ Planck's reduced constant. In the absence of the potential $V(r)$, this equation is easily resolved.$\psi = exp(i\vec{k}\cdot\vec{r})$, here $\vec{k}$ denotes the wave number vector, as well as the magnitude is given by $k = \sqrt{2\mu E/\hbar^2}$. This solution has an asymptomatic in the form [7],

$$\psi \to \frac{i}{2k}\sum_{l=0}^{\infty}(2l+1)\,(i)^l\left(\frac{e^{-ik\left(r-l\pi/2\right)}}{r} - \frac{e^{ik\left(r-l\pi/2\right)}}{r}\right)P_l(\cos\theta) \quad r\to\infty, \qquad (2.8)$$

where θ is the angle between $\vec{r}$ and $\vec{k}$ and P_l are Polynomials of the Legendre. The solution function varies , while the opportunity is present. Nonetheless, the wave function exponential structure can be expressed in a similar way to Eq. (2.8),since potentials vanish at infinity. The exponential structure becomes [7], where the plane waves are replaced by the subsequent Coulomb waves.

$$\psi \to \frac{i}{2k}\sum_{l=0}^{\infty}(2l+1)(i)^l$$

$$\left(\frac{H_l^{(-)}(kr)}{r} - \frac{H_l^{(+)}(kr)}{r}\right)P_l(\cos\theta) \qquad r\to\infty, \qquad (2.9)$$

where $H_l^{(+)}(kr)$ and $H_l^{(-)}(kr)$ they're outgoing and the incoming Coulomb waves, respectively. S_l is the nuclear *S*-matrix and commonly is a complex quantity which we can define. The *S*-matrix is resolved. Expanding the wave function $\psi(\vec{r})$in terms of spherical harmonics as [7] .

$$\psi(\vec{r}) = \sum_{l=0}^{\infty} \sum_{m=-l}^{l} A_{lm} \frac{ul(r)}{r} Y_{lm}(\theta, \phi), \quad (2.10)$$

where A_{lm} is the expansion coefficient, $u_l(r)$ is radial part of the wave function, and $Y_{lm}(\theta, \phi)$ is the spherical harmonics function. The radial part of Schrödinger equation is [7] .

$$\left[-\frac{\hbar^2}{2\mu}\frac{d^2}{dr^2} + V(r) + \frac{l(l+1)\hbar^2}{2\mu r^2} - E\right] u_l(r) = 0, \quad (2.11)$$

where $\frac{l(l+1)\hbar^2}{2\mu r^2}$ represent the centrifugal potential .

The boundary condition can be used to solve the equation, [16] .

$$\begin{aligned} u_l(r) &\sim r^{l+1} && r \to 0 \\ u_l(r) &= H_l^{(-)}(kr) - S_l H_l^{(+)}(kr) && r \to \infty, \end{aligned} \quad (2.12)$$

The nuclear product can be used to calculate the differential elastic cross section. $S - matrix\ S_l$ [57]

$$\frac{d\sigma_{el}}{d\Omega} = |f(\theta)|^2 \quad (2.13)$$

where $f(\theta)$ is the scattering amplitude and is defined as follows: [57] .

$$f(\theta) = \frac{i}{2k} \sum_{l=0}^{\infty} (2l+1)\,(1 - S_l) P_l(cos\,\theta). \quad (2.14)$$

The total elastic cross section is calculated as follows [57]

$$\sigma_{el} = 2\pi \int_{-1}^{1} d(\cos\theta) \frac{d\sigma}{d\Omega} = \frac{\pi}{k^2} \sum_{l=0}^{\infty} (2l+1)|S_l - 1|^2. \quad (2.15)$$

Fusion reactions can be attributed to event flux absorption. When the potential is complex, the S-matrix has a smaller absolute value than when it is simple. Eq(2.9),calculates the difference between the waves coming in and going out [57].

$$j_{in} - j_{out} = \frac{k\hbar}{\mu}\frac{\pi}{k^2}\sum_l (2l+1)(1-|S_l|^2)\,(2l+1) \tag{2.16}$$

The radial flux has been mixed with all possible values of θ in order to obtain Eq(2.16). Taking Eq. (2.16) and dividing it with the incident flux $v = \hbar k/\mu$, the fusion cross section is then written as [57] .

$$\sigma_{fus}(E) = \frac{\pi}{K^2}\sum_l (2l+1)(1-|S_l|^2) \tag{2.17}$$

Before using the common boundary condition at the origin Eq, in heavy-ion fusion reactions. $u_l(r) \sim r^{l+1}$ $r \to 0$ by using the so-called incoming wave boundary condition (IWBC) to save the potential true, the wave function becomes [58] .

$$u_l(r) = T_l\, exp\left(-i\int_{r_{abs}}^{r} k_l(r')dr'\right),\ r \le r_{abs} \tag{2.18}$$

where T_l is probability of tunneling. $k_l(r)$ is a local wave number for the l^{th} partial wave and is referred [58], by distances less than the absorption radius r_{abs} , that is assumed in order to be within the Coulomb barrier.

$$k_r(r) = \sqrt{\frac{2\mu}{\hbar^2}\left(E - V_{(r)} - \frac{\hbar^2 l(l+1)}{2\mu r^2}\right)} \tag{2.19}$$

The incoming wave boundary condition is evaluated when the Coulomb barrier in the inner field consumes a considerable amount of energy and the incoming flux does not return. The choice of absorption radius r_{abs} has no bearing on the outcomes of heavy-ion fusion reactions. r_{abs} are regularly tested to ensure that they are in the best possible condition. (see figure (2.1)). T_l in the Eq. (2.18), for

example, explained as the transmission coefficient using the incoming wave boundary condition. As a result, the reflection coefficient is the *S*-matrix $S_l$in Eq. (2.12). Hence, Eq. (2.17) can be given by [59] .

$$\sigma_{fus}(E) = \frac{\pi}{k^2}\sum_l (2l+1)P_l(E), \tag{2.20}$$

$P_l(E)$ denotes the penetrability of the fusion reaction, which is defined as [60] .

$$P_l(E) = 1 - |S_l|^2 = \frac{k_l\,(r_{abs})}{k}|T_l|^2 \tag{2.21}$$

Coupled channels with absolute angular momentum equation A similar observation applies to quasi-elastic scattering, with cross-sections breaching the Coulomb barrier at collision energies higher than one-dimensional model projections , [60]. The most important nuclear intrinsic movements for heavy-ion collisions have been described as low-lying collective movements, such as low-lying vibrational excitations with multiple multi-polarities or deformed nuclei rotating motion , [61]. The mechanisms of coupling to nucleon transfer also play a part in certain cases [62] .The Hamiltonian for the system [63] .

$$H(\vec{r},\xi) = -\frac{\hbar^2}{2\mu}\nabla^2 + V(r) + H_0(\xi) + V_{coup}(\vec{r},\xi)\ , \tag{2.22}$$

where $H_0(\xi)$is the Hamiltonian for internal motion, $V(r)$ is the bare potential in the absence of the coupling that contains the nuclear and Coulomb components $V(r) = V_N$ (r) + V_C (r), and V_{coup} is the coupling mentioned above. For a complete wave function, the Schrodinger equation becomes [63].

$$\left(-\frac{\hbar^2}{2\mu}\nabla^2 + V(r) + H_0(\xi) + V_{coup}(\vec{r},\xi)\right)\psi(\vec{r},\xi) = E\psi(\vec{r},\xi) \tag{2.23}$$

Fundamentally, the internal degree of freedom has a finite spin. It can be written as [64], which is a multiple of the coupling Hamiltonian.

$$V_{coup}(\vec{r},\xi) = \sum_{\lambda>0,\mu} f_\lambda(r)\, Y_{\lambda\mu}(\hat{r})\, T_{\lambda\mu}(\xi) \tag{2.24}$$

where $f_\lambda(r)$ is redial part of wave function, $Y_{\lambda\mu}(\hat{r})$ is the spherical harmonics in addition $T_{\lambda\mu}(\xi)$ is spherical tensor formed from inner coordinate. A scalar component is represented by the dot except λ = 0, which is already considered in $V(r)$, the sum shall be considered over all values of λ [63] .

$$\langle \vec{r}\xi|(nlI)|JM\rangle = \sum_{m_l m_I}\langle lm_l Im_I|JM\rangle\, Y_{lm_l}(\hat{r})\, \varphi_{n_I m_I}(\xi) \tag{2.25}$$

where the orbital and internal angular momenta are l and I, respectively . $\varphi_{n_I\, m_I}(\xi)$ is the wave function for the internal motion which fulfills [64] .

$$H_0(\xi)\, \varphi_{n_I m_I}(\xi) = \epsilon_n \varphi_{n_I m_I}\,(\xi) \tag{2.26}$$

where ϵ_n is internal energy. The total wave function $\Psi(\vec{r},\xi)$ is developed with this basis as [63] .

$$\psi(\vec{r},\xi) = \sum_{n,l,I}\frac{u^J_{nlI}(r)}{r}\,\langle \vec{r}\xi|(nlI)|JM\rangle\,, \tag{2.27}$$

The Eq(2.23) of Schrödinger is a mathematical formula that describes the behavior of quantum particles. After that, can be written as a series of coupled equations for $u^J_{nlI}(r)$ [64] .

$$\left[-\frac{\hbar^2}{2\mu}\frac{d^2}{dr^2} + V(r) + E + \epsilon_n\right] u^J_{nlI}(r) + \sum_{n'l'I'} V^J_{nlJ;n'l'I'}(r) u^J_{n'l'I'}\,(r) = 0 \tag{2.28}$$

where the coupling matrix elements $V^J_{nlJ;n'l'I'}\,(r)$ are given as [65] .

$$V^J_{nlJ;n'l'I'}\,(r) = \left\langle JM(nlI)\middle|V_{coup}(\vec{r},\xi)\middle|\left(n'l'I'\right)JM\right\rangle \tag{2.29}$$

$$V^J_{nlJ;n'l'I'}\,(r) = \sum_\lambda (-1)^{I-I'+l'+J} f_\lambda(r)\langle l\|Y_\lambda\|l'\rangle\,\langle nI\|T_\lambda\|n'I'\rangle$$
$$\sqrt{(2l\,+\,1)(2I\,+\,1)}\begin{Bmatrix} I' & l' & J \\ l & I & \lambda \end{Bmatrix}. \tag{2.30}$$

Expresses the reduced matrix elements in Eq.(2.30) [66]

$$\langle lm_l|Y_{\lambda\mu}|l'm_{l'}\rangle = \langle l'm_{l'}\lambda\mu\,|lm_l\rangle\,\langle l\|Y_\lambda\|l'\rangle \qquad (2.31)$$

Since $V^J_{nlJ;n'l'I'}(r)$ are unaffected by the index *M*, equation (2.29) named Equations Coupled-Channels since the index has been suppressed as shown in Eq. (2.30). These equations are usually solved using incoming wave boundary conditions for heavy-ion fusion processes, [7] .

$$u^J_{nlI}(r) \sim T^J_{nlI} exp\left(-i\int_{r_{abs}}^{r} K_{nlI}\left(r'\right)d\,r'\right), \qquad r \le r_{abs} \qquad (2.32)$$

$$\rightarrow \frac{i}{2}\left(H_l^{(-)}\right)(k_{nI}r)\delta_{n,n_i}\delta_{l,l_i}\delta_{I,I_i} + \sqrt{\frac{K_{n,I_i}}{K_{nI}}}S^J_{lI}\,H_l^{(+)}(k_{nl}r), \qquad r \to \infty \qquad (2.33)$$

Where $k_{nI} = \sqrt{\frac{2\mu(E\,-\,\epsilon_{nI})}{\hbar^2}}$ and $k_{nI_i} = k = \sqrt{2\mu E/\hbar^2}$ the local wave number k_{nlI} is [67] .

$$k_{nlI}(r) = \sqrt{\frac{2\mu}{\hbar^2}\left(E - \epsilon_{nI} - \frac{l(l+1)\hbar^2}{2\mu r^2} - V(r) - V^J_{nlI;\acute{n}\,l'\acute{I}}(r)\right)}\,. \qquad (2.34)$$

If we have the transmission coefficients, we can proceed with the rest of the process T^J_{nlI}, The penetrability by Coulomb barrier is determined by [68] .

$$P^J_{l_iI_i}(E) = \sum_{n,l,I}\frac{K_{nlI}}{k}\left|T^J_{nlI}\right|^2 \qquad (2.35)$$

Here, $k = k_{n_iI_i}$ is the wave number for the entrance channel. The fusion cross section for un polarized target is known by [68] .

$$\sigma_{fus}(E) = \frac{\pi}{K^2}\sum_{JMl_i}\frac{2J+1}{2I_i+1}P^J_{l_iI_i}(E) \qquad (2.36)$$

When zero is the original intrinsic spin I_i, the initial angular momentum l_i is J . The penetrability is diminished where the indexes l_i and $I_i$are used, eq. (2.36) and then read [68].

$$\sigma_{fus}(E) = \frac{\pi}{K^2}\sum_J (2J+1)P^J(E) \tag{2.37}$$

However, channel couplings had an effect on $P^J(E)$ penetrability. Quasi-elastic cross-section calculations, in contrast to fusion cross-section calculations, require a large angular momentum value to achieve merged values. For such large angular momentum, the potential pocket at $r = r_{abc}$ is minimal. In addition, the incoming flux in Eq. (2.32) can be incorrectly defined. As a result . The quasi-elastic problem commonly employs the conventional boundary conditions at the origin instead of the incoming wave's boundary conditions. Using the standard boundary conditions, $V_N(r) = V_N^0(r) + iW(r)$,a complex potential is needed to simulate the fusion reaction. After finding the nuclear *S*-matrix in Eq. (2.33), the scattering amplitude can be calculated as, where σ_l is the Coulomb phase shift [69] .

$$\sigma_l = \arg\Gamma(l + 1 + i\eta) \tag{2.38}$$

While f_C is the Coulomb scattering amplitude which is given by [52] .

$$f_C(\theta, E) = \frac{\eta}{2k\,sin^2\left(\frac{\theta}{2}\right)} e^{\left[-i\eta In\left(sin^2\left(\frac{\theta}{2}\right)\right)+2i\sigma_0(E)\right]} \tag{2.39}$$

Where is the Sommerfield parameter which is given by $\eta = {Z_1 Z_2 e^2}/{\hbar v}$, the differential cross section is evaluated as [52] .

$$\frac{d\sigma_{qel}(\theta,E)}{d\Omega} = \sum_{JlI}\frac{k_{nI}}{k}\left|f_{lI}^J(\theta,E)\right|^2 \tag{2.40}$$

2.4 Equations of Coupled-Channels in the No-Coriolis Approximation

If several physical channels are detected, Eq (2.30) estimates the maximum coupled-channels, which will be extremely difficult to control. The dimension of the coupled channels equations is usually very large for functional purposes. Since the revolving approximation of the frame or the iso-centrifugal approximation was often used [70], an approximation known as the no-Coriolis approximation is also called, in the field of chemistry, the no-Coriolis approximation was primarily known as centrifugal sudden approximation [71]. The no-Coriolis approximation was first used in chemistry, where it was known as a sudden centrifugal approximation [72]. Assume that the intrinsic spin is zero at the start. In the no-Coriolis approximation, the whole device is converted into a moving frame, with the z-axis pointing in the direction of relative motion in each case. The first angular momentum of the relative motion for each channel is replaced by the overall angular momentum J, which is [7], in the approximation of the rotating frame to the CC equations.

$$\frac{l(l+1)\hbar^2}{2\mu r^2} \approx \frac{J(J+1)\hbar^2}{2\mu r^2} \tag{2.41}$$

As a result of the excitement of the fundamental degree of freedom, this hypothesis suggests that the difference in angular orbital momentum between colliding nuclei is insignificant. As the operator uses relative motion to adjust the rotational coordinate in the space shift with the centrifugal operator

$Y_{\lambda\mu}(\hat{r}=0)=\sqrt{(2\lambda+1)/4\pi}\,\delta_{\mu,0,}$, the coupling Hamiltonian of Eq. (2.24) in the rotating frame reads [73], the transformation to the revolving frame can be used without difficulty.

$$V_{coup}(\vec{r},\xi)=\sum_{\lambda}\sqrt{\frac{(2\lambda+1)}{4\pi}}f_{\lambda}(r)T_{\lambda 0}(\xi) \tag{2.42}$$

In the no-Coriolis approximation, a coiled angular momentum coupling vanishes since a Hamiltonian coupling is no longer reliant on the angular portion of the relative coordinate between colliding nuclei . As a result, the coupled-channel equations are translated into spin-less machine equations. The dimensions of the coupled-channels equations are radically decreased in the no-Coriolis approximation. For instance, for J > 4. When the excitations are terminated at the second excited states, the original coupled-channel equations for quadrupole excitation mode (λ=2) have 13 dimensions. The dimensions are decreased to three in the no-Coriolis approximation. The entire wave function in the rotating frame may be extended to define the coupling-channel equations as in the no-Coriolis approximation [73] .

$$\Psi(\vec{r},\xi) = \sum_{nl} \frac{v_{nl}^{J}(r)}{r} Y_{J0}(\hat{r})\varphi_{nI0}(\xi). \tag{2.43}$$

The (nl)-channel channel radial wave function $v_{nlI}^{J}(r)$is similar to the initial wave function as [74] .

$$u_{nl}^{J}(r) = \sum_{l}\langle I0J0|l0\rangle v_{nlI}^{J}(r). \tag{2.44}$$

The coupled-channels equations for $v_{nl}^{J}(r)$ is then given by [74] .

$$\left[-\frac{\hbar^2}{2\mu}\frac{d^2}{dr^2} + V(r) + \frac{J(J+1)\hbar^2}{2\mu r^2} - E + \epsilon_{nI}\right] v_{nlI}^{J}(r) + \sum_{\acute{n}\acute{l}}\sum_{\lambda>0}\sqrt{(2\lambda+1)/4\pi}$$

$$f_{\lambda}(r)\langle\varphi_{nI}|T_{\lambda\dot{0}}|\varphi_{\acute{n}\acute{l}}\rangle v_{\acute{n}\acute{l}}^{J}(r) = 0 \tag{2.45}$$

These coupling-channel equations are discussed once more using the incoming wave boundary condition for heavy-ion fusion reactions, see (2.32) and (2.33), where $k_{nli}$and $k_{nJI}(r)$are defined in the same way as in the previous subsection. The fusion cross section was gave in Eq. (2.37) where the penetrability is [75].

$$f_{ll}^{J}(\theta,E)=f_{I}^{J}(\theta,E)=i\sum_{J}\sqrt{\frac{\pi}{kk_{nl}}}e^{i[\sigma_J(E)+\sigma_J(E-\epsilon_{nI})]\sqrt{2J+1}\;Y_{J0}(\theta)\left(S_I^J-S_{I,I_i}\right)}$$

$$+f_c(\theta,E)S_{I,I_i} \quad (2.46)$$

We can evaluate the Rutherford cross section [76] .

$$\frac{d\sigma_R(\theta,E)}{d\Omega}=|f_c(\theta.E)|^2=\frac{\eta^2}{4k^2}csc^4\left(\frac{\theta}{2}\right) \quad (2.47)$$

and,

$$\frac{d\sigma_{qel}}{d\sigma_R}(\theta,E)=\sum_{J\ell I}\frac{k_{nI}}{k}\left|\frac{f_{ll}^{J}(\theta,E)}{f_c(\theta.E)}\right|^2 \quad (2.48)$$

Several reviews have looked at the legality of the no-Coriolis approximation for both quasi-elastic scattering and the heavy-ion fusion reaction, and it seems that this approximation works well [61] .

2.5 Nuclear Coupling

The basic form of Hamiltonian coupling V_{coup} is studied in this thesis. It's assumed that the nuclear potential follows the Woods-Saxon formula (Eq (2.3). Let's start with couplings of relative motion to the 2-poles surface vibration of the target nucleus. In the Bohr and Mottelson geometrical model, the radius of the target vibrating nucleus is defined as [77] .

$$R_T(\theta,\phi)=R_T\left(1+\sum_\lambda\alpha_{\lambda\mu}Y_{\lambda\mu}(\theta,\phi)\right) \quad (2.49)$$

R_T is the comparable sharp radius whereas $\alpha_{\lambda\mu}$is the surface vibration coordinate. A harmonic oscillator can be worked approximately to the surface oscillation and is provided by [77] .

$$H_0=\hbar\omega_\lambda\left(\sum_\mu a_{\lambda\mu}^{\dagger}a_{\lambda\mu}+\frac{2\lambda+1}{2}\right) \quad (2.50)$$

where $\hbar\omega_\lambda$is the oscillator quanta and $a^\dagger_{\lambda\mu}$ and $a_{\lambda\mu}$ are the phonon creation and annihilation operators, respectively. The surface coordinate $\alpha_{\lambda\mu}$ is related to the phonon creation and annihilation operators by :

$$\alpha_{\lambda\mu} = \alpha_0\left(a^\dagger_{\lambda\mu} + (-1)^\mu a_{\lambda\mu}\right) \tag{2.51}$$

α_0 is the amplitude of the zero point motion and is connected to the deformation parameter β_λ by $\alpha_0 = \beta_\lambda \Big/ \sqrt{2\lambda+1}$. The deformation parameter β_λ can be calculated using the gauged probability of electromagnetic transformation $B(E\lambda)\uparrow$ by using [77] .

$$\beta_\lambda = \frac{4\pi}{3Z_T R_C^\lambda}\left[\frac{B(E\lambda)\uparrow}{e^2}\right]^{\frac{1}{2}}. \tag{2.52}$$

where R_C is the Coulomb radius, and is needed to be the same as R_T.Therefore, α_0 is given by [78] .

$$\alpha_0 = \frac{1}{\sqrt{2\lambda+1}}\frac{4\pi}{3Z_T R_C^\lambda}\left[\frac{B(E\lambda)\uparrow}{e^2}\right]^{\frac{1}{2}} \tag{2.53}$$

In the no-Coriolis approximation, the relative motion's angular momentum remains unchanged . A factor $\sqrt{2\lambda+1/4\pi}$ is obtained by evaluating related spherical harmonics in Eq (2.49) by angle $\hat{\boldsymbol{r}}$ = 0. As a result [78], published Eq. (2.49)

$$R_T(\theta, \alpha_{\lambda 0}) = R_T\left(1 + \sqrt{2\lambda+1/4\pi}\,\alpha_{\lambda 0}\right). \tag{2.54}$$

A formula for the nuclear coupling potential,[79] .

$$V_N^{coup(vib)}\left(r, \hat{O}_\lambda\right) = \frac{-V_o}{1+e^{\left[r-R_0-R_T\hat{O}_{\lambda'}\backslash a\right]}}, \tag{2.55}$$

where $\hat{O}_\lambda$ is the dynamical operator [80] .

$$\hat{O}_\lambda = \beta_\lambda\left(a^\dagger_{\lambda 0} + a_{\lambda 0}\right). \tag{2.56}$$

To obtain matrix elements of a Hamiltonian nuclear coupling, the eigenvalues and eigenvectors must be determined. Between the n-phonon and the m-phonon states. Operator $\hat{O}_\lambda$ is looking for a way to satisfy [80].

$$\hat{O}_\lambda|\alpha\rangle = \xi_\alpha|\alpha\rangle \tag{2.57}$$

The eigenvalues and eigenvectors of the operator between phonon states can be obtained by diagonalizing the matrix elements of the operator [81] .

$$O_{nm} = \beta_\lambda\left(\sqrt{m}\,\delta_{n,m-1} + \sqrt{m+1}\delta_{n,m+1}\right) \tag{2.58}$$

Since the eigenvalues and eigenvectors have been checked, the nuclear matrix elements of Eq. (2.55) it's calculated and written as [81].

$$V^N_{mn}(r) = \left\langle m\left|V_N^{coup(vib)}\right|n\right\rangle - V_N(r)\delta_{n,m}.$$

$$= \sum_\alpha \langle m|\alpha\rangle\,\langle\alpha|n\rangle \frac{-V_o}{1+e^{[r-R_0-R_T\xi_\alpha/\sqrt{4\pi}/\alpha]}} - V_N(r)\delta_{n,m}. \tag{2.59}$$

The last term in Eq. (2.59) is presented to ensure that the coupling relationship in the admission channel vanishes.

2.6 Coupling of Coulomb

We can describe the Coulomb potential between a point-like spherical projectile and a vibrating target [82] .

$$V_C(\vec{r}) = \int d\vec{\acute{r}}\,\frac{Z_p Z_T e^2}{\left|\vec{r}-\vec{\acute{r}}\right|}\rho_T\left(\vec{\acute{r}}\right)$$

$$= \frac{Z_p Z_T e^2}{r} + \sum_{\lambda\neq 0}\sum_{\acute{\mu}} \frac{4\pi Z_P e}{2\acute{\lambda}+1} Q_{\acute{\lambda}\acute{\mu}} Y^*_{\acute{\lambda}\acute{\mu}}(\hat{r})\,\frac{1}{r^{\acute{\lambda}+1}}, \tag{2.60}$$

where ρ_T denotes the target nucleus' charge density, Z_T denotes the target's atomic number, and Z_P denotes the projectile nucleus' atomic number, and $Q_{\acute{\lambda}\acute{\mu}}$denotes the electric multipole operator described by [83] .

$$Q_{\acute{\lambda}\acute{\mu}} = \int d\vec{r}\, Z_T e\, \rho_T(\vec{r})\, r^{\acute{\lambda}}\, Y_{\acute{\lambda}\acute{\mu}}(\hat{r}) \tag{2.61}$$

The bare potential of Coulomb is on the right-hand side of Eq, the first concept (2.60), while the part of the Hamiltonian coupling is the second term. The formula below is used to generate Eq (2.60) [84] .

$$\frac{1}{\left|\vec{r}-\vec{\acute{r}}\right|} = \sum_{\lambda\acute{\mu}} \frac{4\pi}{2\acute{\lambda}+1} \frac{r_<^{\acute{\lambda}}}{r_>^{\acute{\lambda}+1}} Y_{\acute{\lambda}\acute{\mu}}(\hat{\acute{r}}) Y^*_{\lambda\acute{\mu}}(\hat{r}) \tag{2.62}$$

If the charge radius of the target nucleus is assumed to be greater than the relative coordinate r, the electric multi pole is taken by, assuming a sharp distribution of matter for the target nucleus [85].

$$Q_{\acute{\lambda}\acute{\mu}} = \frac{3Z_T e}{4\pi} R_T^{\acute{\lambda}}\, \alpha_{\lambda\mu} \delta_{\lambda,\acute{\lambda}} \delta_{\mu,\acute{\mu}}. \tag{2.63}$$

Therefore, It can create the coupling part of the Coulomb interaction as the first order in the surface coordinate $\alpha_{\lambda\mu}$ [52] .

$$V_C^{coup(vib)}(r, \alpha_{\lambda\mu}) = \sum_{\lambda\acute{\mu}} \frac{3Z_P Z_T e^2}{2\acute{\lambda}+1} \alpha_{\lambda\mu} Y^*_{\lambda\acute{\mu}}(\hat{r}) = \sum_{\lambda\mu} f_\lambda^C(r) \alpha_{\lambda\mu} Y^*_{\lambda\acute{\mu}}(\hat{r}) \tag{2.64}$$

where,

$$f_\lambda^C(r) = \frac{3Z_P Z_T e^2}{2\acute{\lambda}+1} \frac{R_T^{\acute{\lambda}}}{r^{\acute{\lambda}+1}} \tag{2.65}$$

The Coulomb coupling's type factor is defined as, the Coulomb coupling is calculated by converting a rotating frame using the no-Coriolis approximation, and it is written as [86] .

$$V_C^{coup(vib)}(r, \alpha_{\lambda\mu}) = \sum_\lambda 3Z_P Z_T e^2 \frac{R_T^{\acute{\lambda}}}{r^{\acute{\lambda}+1}} \frac{\alpha_{\lambda 0}}{\sqrt{4\pi}} = \sum_\lambda \frac{3Z_P Z_T e^2}{2\acute{\lambda}+1} \frac{R_T^{\lambda}}{r^{\acute{\lambda}+1}} \frac{\hat{O}_\lambda}{\sqrt{4\pi}} \tag{2.66}$$

where is $\widehat{O}_\lambda$ given by Eq. (2.56). The Coulomb coupling matrix elements, denoted by $V_{nm}^{C}(r)$, can after that be calculated similar to the nuclear coupling Hamiltonian, with

$$V_{nm}^{C}(r) = \left\langle m \middle| V_N^{coup(vib)}(r) \middle| n \right\rangle = \sum_\lambda \frac{3Z_P Z_T e^2}{2\acute{\lambda}+1} \frac{R_T^\lambda}{r^{\acute{\lambda}+1}} \frac{\beta_\lambda}{\sqrt{4\pi}} \left[\sqrt{m}\delta_{n,m-1} + \sqrt{m+1}\delta_{n,m+1}\right] \quad (2.67)$$

The complete coupling matrix components are primarily the number of nuclear and Coulomb couplings [86] .

$$V_{coup}(r) = V_{mn}^{N}(r) + V_{nm}^{C}(r) \quad (2.68)$$

Chapter Three

Results, Discussion , Conclusions and Future Work

3.1 Introduction

In the present study, several programs were used, among which we mention CQEL, chi-square codes and so used other programs to help in calculations such as GRAPHER and GET DATA. The important code is used in SC and CC calculations are CQEL program [7] and which is concerned with the Schrödinger equation and the coupling equations [87]. The chi-square method was used to evaluate the factor between the theoretical approximation and the experimental results [7] . The deformation parameters are used to classify the excited states in a rotational or vibrational model. The number of included states can be specified specifically for rotational states, while multi-phonon interactions can be included for vibrational states. It is possible to have all reciprocal relations between various vibrational states in the target and projectile. In the other hand, including transition processes to chosen states in the residual projectile and targets such as nuclei is not possible. However, there is a simple way to include one transfer channel [7] , for more information. The nuclear potential is assumed to have a Woods-Saxon configuration in this thesis. The nuclear potential was calculated using the WS model, which has real and imaginary components. The nuclear potential of the surface area is defined by the diffusion parameter [88]. $R_T = r_{0T}A^{\frac{1}{3}}$ was used to determine the target's radius, thus $r_0 = 1.2$ fm ,and $R_p = r_{0p}A^{\frac{1}{3}}$. The nuclear potential of systems ^{6}Li + ^{64}Zn, ^{23}Na+ ^{90}Zr, ^{11}C + ^{208}Pb, ^{16}O+ ^{208}Pb, and ^{16}O+ ^{63}Cu is investigated using quasi-elastic scattering in this study as will be detailed in this chapter.

3.2 Results and Discussion

3.2.1 ^{6}Li + ^{64}Zn System

The diffuseness parameter for ^{6}Li + ^{64}Zn system was discussed in five cases, which we considered in the first case the projectile ^{6}Li as well as target ^{64}Zn as inert nuclei (SC) with values of the diffuseness parameter $a_0 = (0.66, 0.63, 0.60)$ fm, also in the second case, we considered the projectile ^{6}Li as inert coupling while target ^{64}Zn nucleus is rotational coupling with deformation parameter $\beta_2 = 0.219$ [89] with the value of the diffuseness parameter $a_0 = 0.63$ fm. In the last case, we assumed target ^{64}Zn as rotational coupling nuclei with value of the diffuseness parameter $a_0 = 0.66$ fm with deformation parameter $\beta_2 = 0.219$ [89] and the projectile ^{6}Li as inert nuclei, respectively, by $E_{c.m.} = 17.25$ MeV. and the potential depth $V_0 = 8.5$ MeV and the radius parameter $r_0 = 1.1$ fm.

In Table 3.1, the diffuseness parameters (a), as well as other WS potential characteristics and values of χ^2 fitting between experimental and theoretical data for the ^{6}Li + ^{64}Zn reaction, were derived using SC and CC analyses.

Table 3.1: Woods-Saxon potential parameters and Energy center of mass for all orders of coupling in ^{6}Li + ^{64}Zn nuclear reactions.

System	Case	V_0 (MeV)	r_0 (fm)	a_0 (fm)	$E_{c.m.}$(MeV)	χ^2
^{6}Li + ^{64}Zn	Single channel	8.5	1.1	0.66	17.25	0.00030
				0.63		0.00018
				0.60		0.00012
	Inrt. + Rot.	8.5	1.1	0.63	17.25	0.00017
	Inrt + Rot.			0.66		0.00031

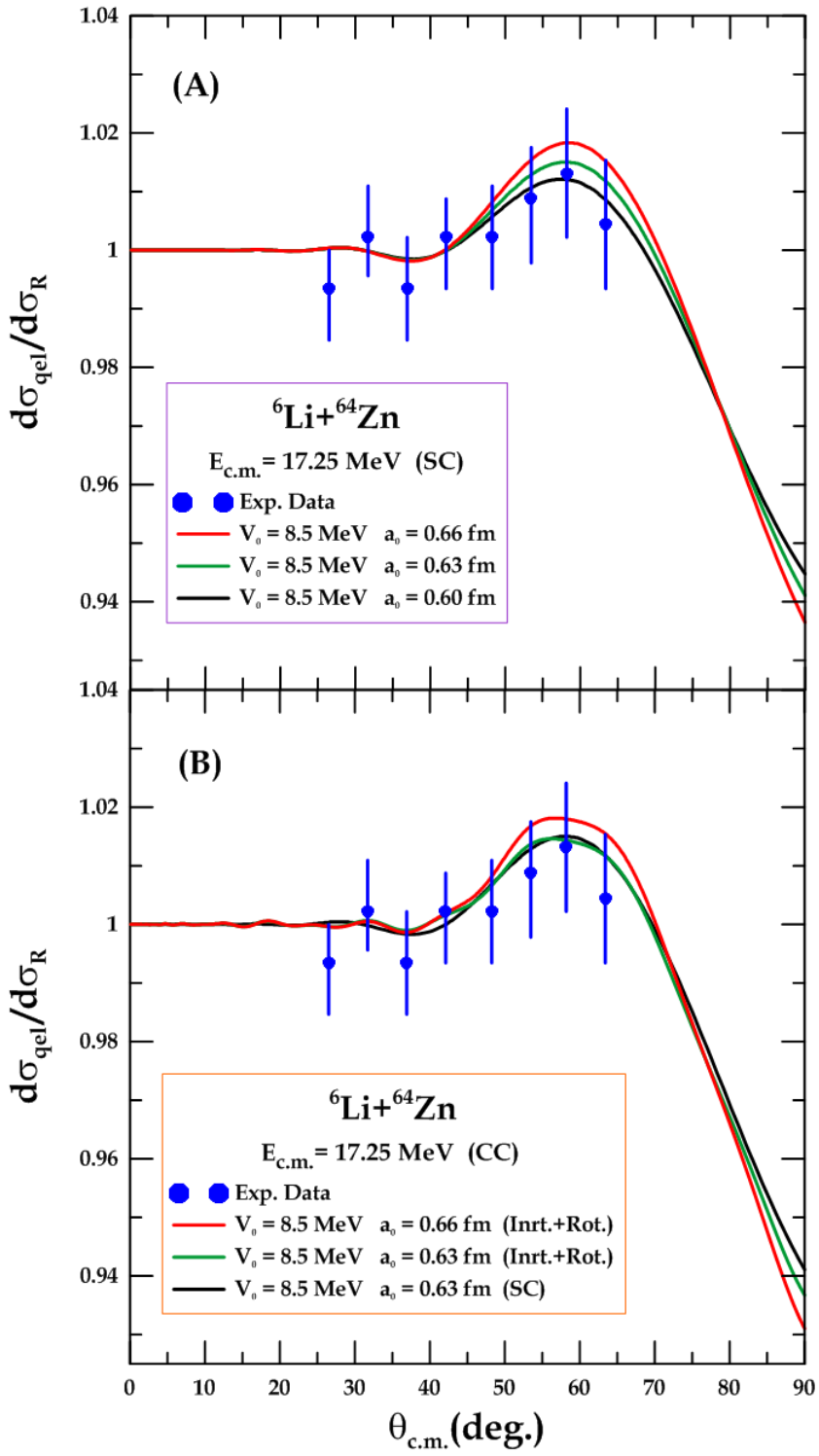

Figure 3.1: Comparison of SC and different types of CC calculations Quasi elastic scattering with experimental data (referred to as points with error bars) from Ref.[90] for ^{6}Li + ^{64}Zn system: panel (A) Single channel case, a red, green and black curves at $a_0 = (0.66, 0.63, 0.60)$ fm, respectively, panel (B) Coupled channel (Inrt.+Rot. and Inrt.+Rot.), a red and green curve at $a_0 = (0.66, 0.63)$ fm. respectively, at $E_{c.m.} = 17.25$ MeV, blue circles represent experimental data .

Figure 3.1 shows the better-fitted value of the diffusenes parameter has been obtained from SC analysis in ^{6}Li + ^{64}Zn system is 0.60 fm, with χ^2 =0.00012. The better-fitted diffuseness parameter is in accordance with the standard value of about 0.63 fm, that' s represented by the black line in Fig 3.1(A)

The best-fitted value of the diffuseness parameter taken through a calculation of coupled-channels CC is 0.63 fm, with χ^2=0.00017 . This is shown in Figure 3.1(B) with the red solid line .

CC analyzes with inert projectile and target as rotational have produced the most suitable value of the diffuseness parameter a= 0.63 fm, considered fully consistent with the standard value.

Ultimately, we could have compared between the result of $d\sigma_{qel}/d\sigma_R$, which has been obtained using SC analysis at the best suitable value of the diffuseness parameter a= 0.63 fm with χ^2=0.00018 (represented by the green line in Fig 3.1(a)) and the best suitable value of the diffuseness parameter 0.63 fm with χ^2=0.00017 which has been obtained from CC analysis (represented by the red line in Fig 3.1(B)).

In addition, the resulting χ^2 values indicate that the uniquely fit diffuseness parameter taken via a coupled-channel measurement matches the experimental data very well from the one obtained through a measurement of a coupled channel, when the inert projectile and rotational target coupling .

The largest effect in this system comes from the target, to obtain the best-fitted diffuseness parameter, the projectile must be inert. When we employed complete CC calculations, this framework saved us a lot of time and avoided us from getting into a complicated mathematical difficulty.

3.2.2 ^{23}Na+ ^{90}Zr System

The diffuseness parameter was discussed for ^{23}Na + ^{90}Zr system in cases where we assumed the projectile ^{23}Na and target ^{90}Zr as inert nuclei (SC) with diffuseness parameter values a_0 = (0.65, 0.63, 0.61) fm respectively. Another case described target ^{90}Zr as a quadrupole vibrational nucleus with parameter deformation β_0= 0.035 [89] to the state 2^+ (2.186274 MeV), with value of the diffuseness parameter $a_0 = 0.63$ fm and the projectile ^{23}Na as inert nuclei. For the last case, target ^{90}Zr to be a quadrupole vibrational nucleus [89] to the, with value of the diffuseness parameter $a_0 = 0.61$ fm whereas the projectile nucleus ^{23}Na is inert, single phonon and the radius parameter $r_0 = 1.1$ fm, and the potential depth $V_0 = 86.5$ MeV by $E_{c.m.} = 87.6$MeV.

In Table 3.2, the diffuseness parameters (a), as well as other WS potential parameters and values of χ^2 fitting between experimental and theoretical data for the ^{23}Na + ^{90}Zr reaction, were derived using SC and CC analyses.

Table 3.2: Woods-Saxon potential parameters and Energy center of mass for all orders of coupling in ^{23}Na + ^{90}Zr nuclear reactions

System	Case	V_0 (MeV)	r_0 (fm)	a_0 (fm)	$E_{c.m.}$(MeV)	χ^2
^{23}Na + ^{90}Zr	Single channel	86.5	1.1	0.65	87.6	0.12268
				0.63		0.19833
				0.61		0.29390
	Inrt + Vib	86.5	1.1	0.63	87.6	0.19671
				0.61		0.29200

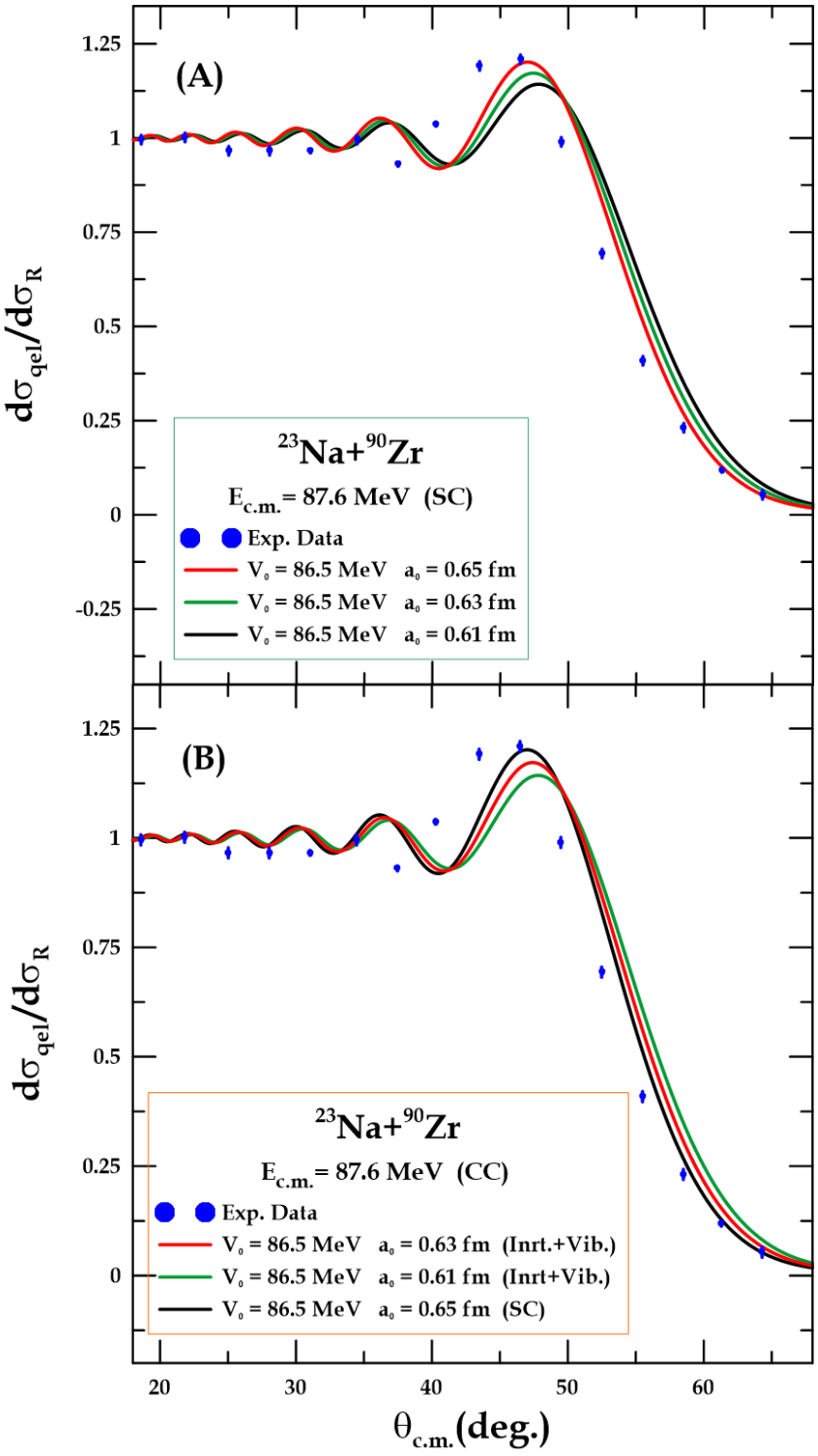

Figure 3.2 : Comparison of SC and different types of CC calculations Quasi elastic scattering with experimental data (referred to as points with error bars) from Ref.[91] for ^{23}Na + ^{90}Zr system, a red, green and black curves at $a_0 = (0.65, 0.63, 0.61)$ fm respectively, panel (A) Single channel case, and panel (B) Coupled channel (Inrt + Vib.) by $E_{c.m} = 87.6$ MeV, blue circles represent experimental data .

Results in Table (3.2) show the best suitable value of the diffuseness parameter which has been obtained from SC analysis, is 0.65 fm with χ^2=0.12268, this value is considered very near for standard value 0.63 fm, which is represented by the red line in Fig.3.2(A) by V_0 = 86.5 MeV and

$E_{c.m} = 87.6$ MeV .

The better-fitted diffuseness parameter for a coupled-channel calculations shall be 0.63 fm, with χ^2 = 0.19671 and V_0 = 86.5 MeV. The best-fitted diffuseness parameter, which is (shown by the red line in figure (3.2(B)) is in perfectly match with the standard value.

The best value of the diffuseness parameter a=0.63 fm with χ^2 =0.19833 was given from SC (represented by green line Fig 3.2(A)) and CC analyzes with vibrational target and inert projectile with χ^2 =0.19671 (represented by red line Fig 3.2(B)), which is assumed to be completely consistent with the calculated value, while the projectile is inert to give the best-fitted diffuseness parameter . Looking at the figure (3.2) panel (A) and (B) it is noted that there is a convergence between them, which was shown by the calculations SC and CC and small values of χ^2 due to the small value of the parameter distortion, whose value is, whose value is β_0= 0.035 [89].

3.2.3 ^{11}C + ^{208}Pb System

The diffuseness parameter was discussed in the ^{11}C + ^{208}Pb system in five case: in the first, second and third case, we considered the projectile ^{11}C and target ^{208}Pb to be inert nuclei (SC) with diffuseness values a_0=(0.67, 0.64, 0.61) fm correspondingly, and potential depth $V_0 = (320,\ 325,\ 330\ )$MeV, respectively. In the fourth case, the projectile ^{11}C suppose as inert nuclei, and considered target ^{208}Pb to be a quadruple vibrational nucleus with deformation parameter $\beta_0 = 0.055$ [89] to the state 2^+ (4.0854 MeV), with the value of the diffuseness parameter $a_0 = (0.67)$ fm the potential depth $V_0 = 320$ MeV. In

the last case, we considered target ^{208}Pb is vibrational coupling whereas the projectile^{11}C is inert with values of the diffuseness parameter $a_0 = 0.64$ fm, and $V_0 = 325\text{MeV}$ with single phonon in and the radius parameter $r_0 = 1.2$fm by $E_{c.m.} = 226.0$ MeV.

In Table 3.3, the diffuseness parameters (a), as well as other WS potential characteristics and values of χ^2 fitting between experimental and theoretical data for the ^{11}C + ^{208}Pb reaction, were derived using SC and CC analyses.

Table 3.3 : Woods-Saxon potential parameters and energy center of mass for all orders of coupling in ^{11}C + ^{208}Pb nuclear reactions

System	Case	V_0 (MeV)	r_0 (fm)	a_0 (fm)	$E_{c.m.}$(MeV)	χ^2
^{11}C + ^{208}Pb	Single Channel	320	1.2	0.67	226.0	0.17073
		325		0.64		0.35031
		330		0.61		0.39498
	Inrt + Vib.	320	1.2	0.67		0.23239
		325		0.64		0.26646

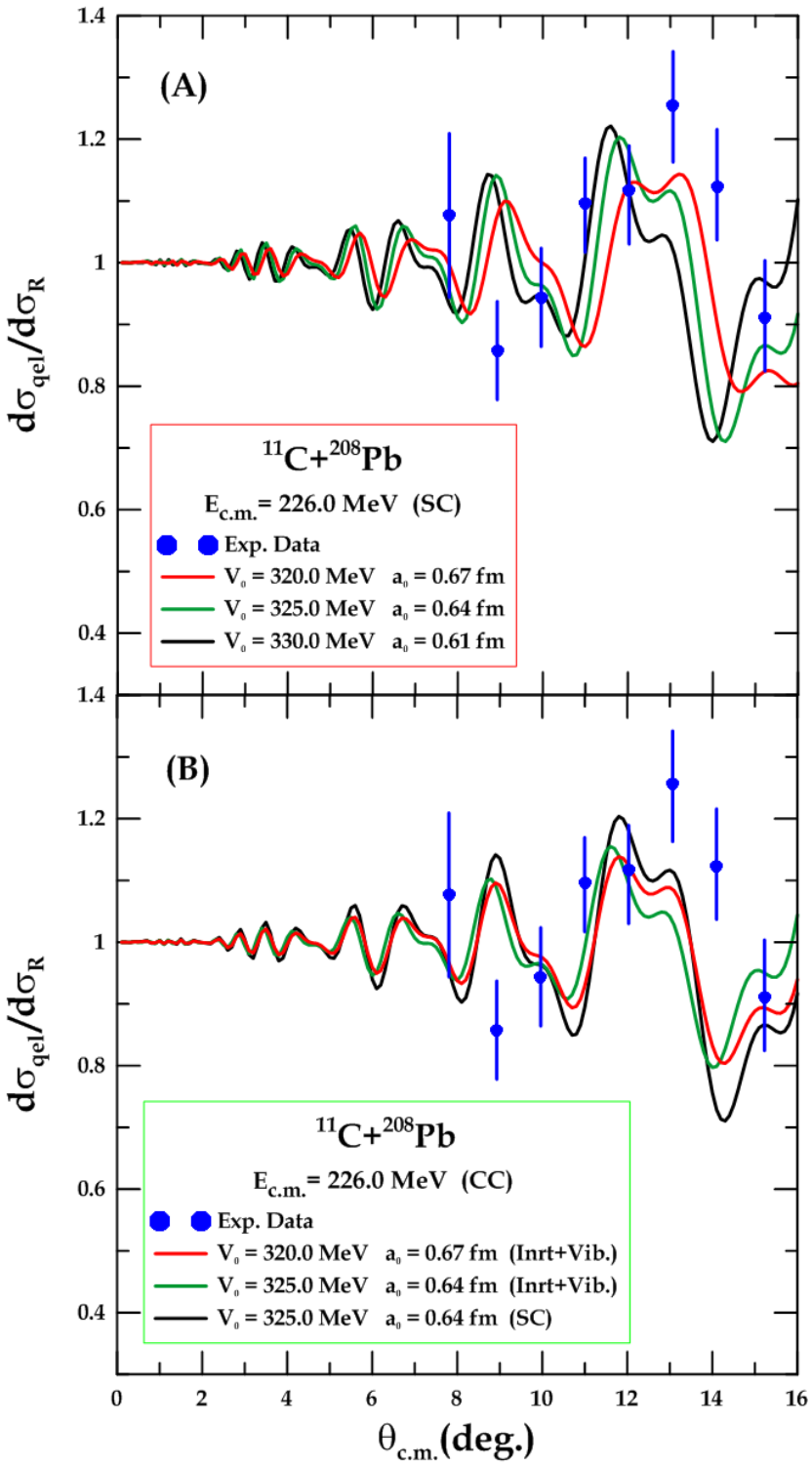

Figure 3.3 : Comparison of SC and different types of CC calculations Quasi elastic scattering with experimental data (referred to as points with error bars) from Ref,[92] for ^{11}C + ^{208}Pb system: panel (A) Single channel case a red, green and black curves at $a_0 = (0.67, 0.64, 0.61)$ fm respectively, and panel (B) Coupled channel (Inrt.+Vib.), a red and green curves at $a_0 = (0.67, 0.64)$ fm. respectively, by $E_{c.m.} = 226$ MeV, blue circles represent experimental data .

Figure 3.3 show the excellent matched diffuseness parameter is obtained by using a single-channel technique for ^{11}C + ^{208}Pb system is 0.67 fm, with χ^2 = 0.17073 and V_0 = 320.0 MeV, presents the quasi-elastic ratio measured to the Rutherford cross sections for a_0 = 0.67 fm calculation with a single channel. A coupled-channels calculation revealed that the best-suited diffuseness parameter is 0.67 fm, as illustrated by the red line in Figure (3.4 (B)),with χ^2 = 0.23239 and V_0 = 320.0 MeV. Once again, the resulting χ^2 values suggest that the well-fitted diffuseness parameter acquired through a coupled-channels study can improve on the experimental data acquired from a single-channel study.

The best suitable value of the diffuseness parameter which has been obtained value a_0 = 0.67 fm has been found from SC analyses and CC analyses with inert target and vibrational projectile (as Figure 3.3), that is higher compared to the standard value . Such investigations the improved performance compared to similar system results, where vibrational systems were discussed to be the projectile and target. Hence, the greatest effect in this system comes from the projectile.

3.2.4 ^{16}O+ ^{208}Pb System

The diffuseness parameter was discussed in the ^{16}O + ^{208}Pb system in five cases: in the first, second and third cases, we considered the projectile ^{16}O and target ^{208}Pb to be inert nuclei (SC) with diffuseness values a_0=(0.67, 0.63, 0.59) fm correspondingly, and potential depth $V_0 = 80.9 MeV$. In the fourth case, we considered target ^{208}Pb to be a quadruple vibrational nucleus with deformation parameter $\beta_0 = 0.055$ [89] to the state 2^+ (4.0854 MeV), with the value of the diffuseness parameter $a_0 = (0.67)$ fm the potential depth $V_0 =$ 80.9 MeV , and the projectile nucleus ^{16}O is a quadruple vibrational nucleus with deformation parameter $\beta_0 = 0.364$ [89] to the state 2^+ (6.917MeV) with values of the diffuseness parameter $a_0 = 0.61$ fm. In the last case, we presumed

target ^{208}Pb is vibrational coupling whereas the projectile ^{16}O is inert with values of the diffuseness parameter $a_0 = 0.67$ fm by $E_{c.m.} = 96.0$ MeV and the radius parameter $r_0 = 1.2$ fm were appeared in Table 3.4.

In Table 3.4, the diffuseness parameters (a), as well as other WS potential characteristics and values of χ^2 fitting between experimental and theoretical data for the ^{16}O + ^{208}Pb reaction, were derived using SC and CC analyses.

Table 3.4: Woods-Saxon potential parameters and Energy center of mass for all orders of coupling in ^{16}O + ^{208}Pb nuclear reactions

System	Case	V_0 (MeV)	r_0 (fm)	a_0 (fm)	$E_{c.m.}$(MeV)	χ^2
^{16}O + ^{208}Pb	Single channel	80.9	1.2	0.67	96.0	0.01886
				0.63		0.02079
				0.59		0.02955
	Vib. + Vib.	80.9	1.2	0.61	96.0	0.01936
	Inrt +Vib.			0.67		0.04642

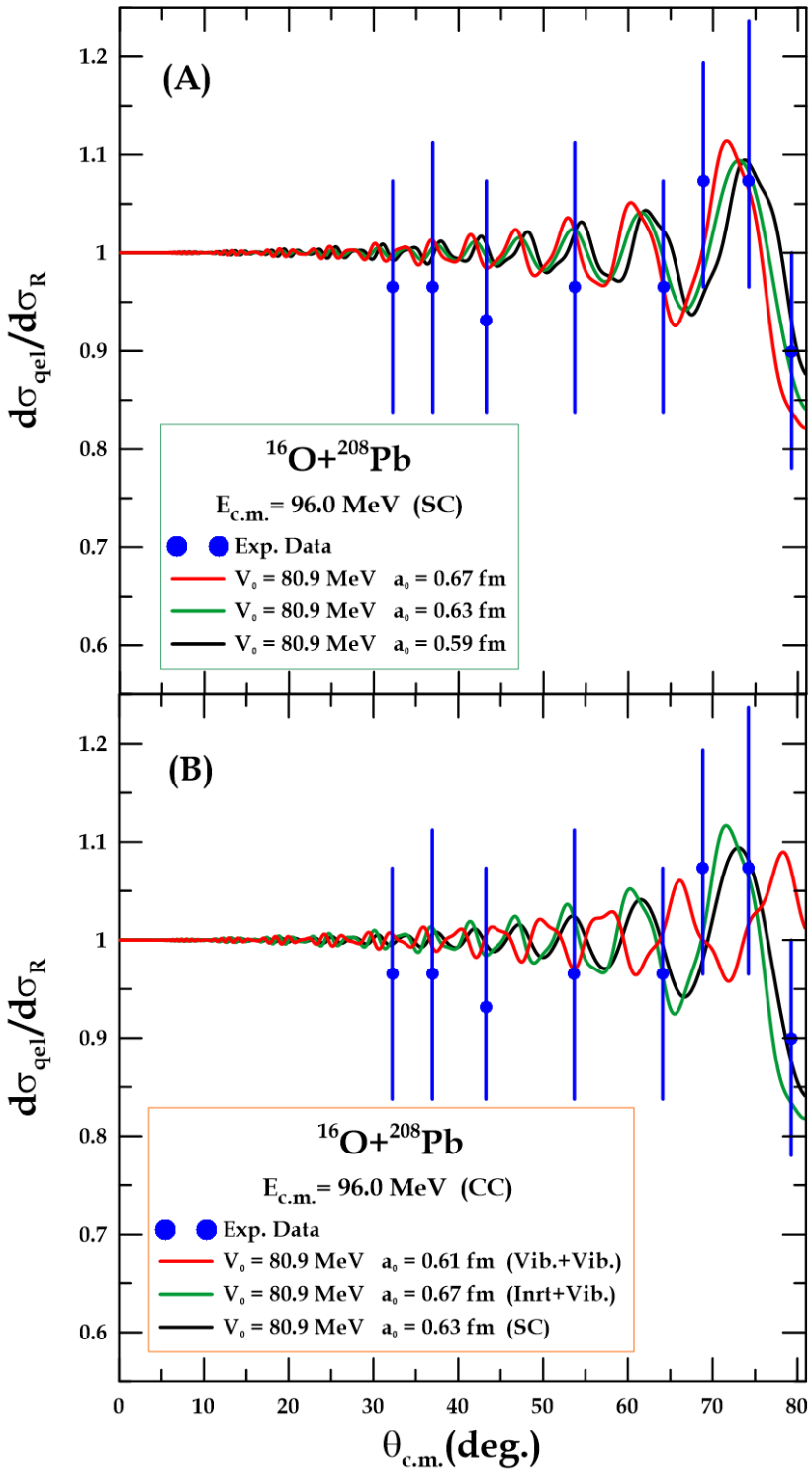

Figure 3.4 : Comparison of SC and different types of CC calculations Quasi elastic scattering with experimental data (referred to as points with error bars) from Ref [93] for ^{16}O + ^{208}Pb system : (A) Single channel case ,a red , green and black curves at $a_0 = (0.67, 0.63, 0.59)$ fm and (B) Coupled channel (Vib + Vib.) a red curve at $a_0 = 0.61$ fm ,(Inrt +Vib) at $a_0 = 0.67$ fm by $E_{c.m.} =$ 96.0 MeV, the blue circles represent experimental data .

Results in Table 3.4 show we could compare the result of $d\sigma_{qel}/d\sigma_R$, which has been obtained using SC analysis. The best suitable diffuseness parameter for the $^{16}O+ ^{208}Pb$ system obtained by a single-channel explanation is 0.67 fm , χ^2 value is 0.01886 with the red line in Figure 3.4- A had shown the best - fitting diffuseness parameter for the $^{16}O + ^{208}Pb$ system. (3.4 (A), (B)) and the result determined by means of a CC analysis if the projectile and the target are vibrational coupled at the good value of the diffuseness parameter a_0 = 0.61 fm with χ^2 value is 0.01936, and the potential depth V_0 needed for reproducing the height of the barrier is 80.9 MeV. Figure (3.4 (B)) indicates the measured quasi-elastic ratio to the Rutherford cross sections for a_0 = 0.61 fm using the approximation of a coupled channels.

CC analysis results with inert projectile and vibrational target (in Figure 3.4) have given the highest suitable value for the diffuseness parameter a_0 = 0.67fm which is assumed entirely to be in consistent with the standard value. Such analyzes improved performance as compared to the performance of similar systems where the projectile and target are, respectively, called vibrational and rotational systems. Subsequently, the greatest effect in such systems comes from the target whilst projectile is inert to obtain the better-suited diffuseness parameter.

3.2.5 $^{16}O+ ^{63}Cu$ System

In $^{16}O+ ^{63}Cu$ system, the diffuseness parameter was evaluated in five cases, where we considered in the first case projectile ^{16}O also the target ^{63}Cu as inert nuclei (single channel SC) as show in fig (3.5A) with the value of the diffuseness parameter a_o= (0.65) fm with the potential depth $V_0 = 35.5$ MeV . In the second case, a_o= (0.63) fm with the potential depth $V_0 = 37.5$ MeV .In the third case, a_o= (0.61) fm with the potential depth $V_0 = 39.5$ MeV .In the third case we considered quadruple vibrational nucleus with deformation

parameter $\beta_0 = 0.364$ [89] to the state 2^+ (6.917 MeV), projectile ^{16}O with inert target ^{63}Cu ,the coupling to this state nuclei with the diffuseness parameter's value $a_0 = 0.61$ fm, the potential depth $V_0 = 39.5$ MeV ,and last case, we assumed target ^{63}Cu nucleus as an inert coupling nuclei with value of the diffuseness parameter $a_0 = (0.65)$ fm, the potential depth $V_0 = 35.5$ MeV , the radius parameter $r_0 = 1.2$ fm and the center of mass energy $E_{c.m.} = 64.0$ MeV.

In Table 3.5, the diffuseness parameters (a), as well as other WS potential parameters and values of χ^2 fitting between experimental and theoretical data for the ^{16}O + ^{63}Cu reaction, were derived using SC and CC analyses.

Table 3.5: Woods-Saxon potential parameters and energy center of mass for all orders of coupling in ^{16}O + ^{63}Cu nuclear reactions.

System	Case	V_0 (MeV)	r_0 (fm)	a_0 (fm)	$E_{c.m.}$(MeV)	χ^2
^{16}O + ^{63}Cu	Single Channel	35.5	1.2	0.65	64.0	0.10548
		37.5		0.63		0.11180
		39.5		0.61		0.11036
	Vib. + Inert.	39.5		0.61		0.10580
		35.5		0.65		0.11004

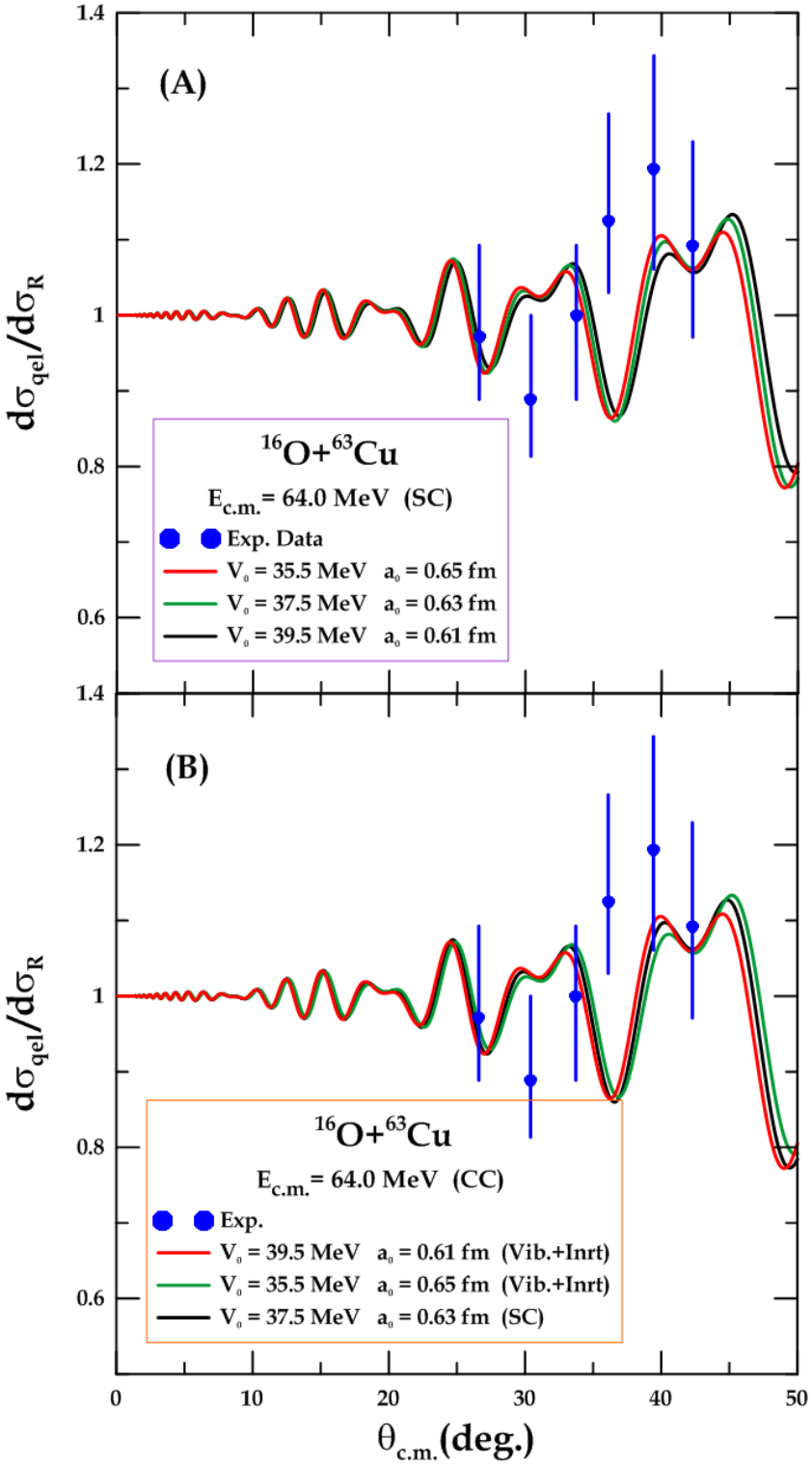

Figure 3.5 : Comparison of SC and different types of CC calculations Quasi elastic scattering with experimental data (referred to as points with error bars) from Ref [93] for ^{16}O + ^{63}Cu system: (A) Single channel case, a red, green and black curves at $a_0 = (0.65, 0.63, 0.61)$ fm respectively, and (B) Coupled channel (Vib.+ Inert.), a red and green curves at $a_0 = (0.61, 0.65)$ fm respectively, by $E_{c.m.} = 64$ MeV, blue circles represent experimental data .

For $^{16}O+ ^{63}Cu$ system, results in Table 3.5 show the best-suited diffuseness parameter taken by measuring a single channel is 0.65 fm, with χ^2 = 0.10548 and V_0=35.5 MeV. The red line in Figure (3.5 (A)) show the best-fit diffuseness, which is quite close to the fundamental value. This may be observed in the results of various collision systems, where coupled channel calculations offer a better match for the experimental data than single channel simulations . The best-fitted diffuseness parameter is 0.61 fm by using coupled-channel approach, with χ^2 = 0.10580 and V_0= 39.5 MeV.

CC analyzes with inert target and vibrational projectile obtained the best suitable value for the diffuseness parameter a_0 = 0.61 fm, are considered entirely consistent with the standard value. In addition, the greatest effect in such systems comes from projectile, whilst target is inert to achieve the perfectly matched diffuseness parameter.

3.3 Conclusions

We may deduce the following remarks based on the data and final conclusions presented in Tables (3.1,2,3,4,5) for all systems researched in this thesis.:

1. The best fitted the diffuseness parameters for $^{6}Li + ^{64}Zn$, $^{23}Na + ^{90}Zr$, $^{11}C + ^{208}Pb$, $^{16}O+ ^{208}Pb$, and $^{16}O + ^{63}Cu$ systems are compatible compared with the standard value 0.63 fm.
2. The diffuseness parameters in(CC) case with the best match for $^{6}Li + ^{64}Zn$ systems relative to the regular value of 0.63 fm are totally compatible.
3. The system's rotational coupling system was able to perform theoretical calculations with greater success than the vibration coupling with another approach for simulating experimental data.

4. The coupling for the choose structures decreased the coefficients of diffusion derived from SC analyses.
5. The SC analysis, which ranged from (0.59-0.67) fm for all systems, gained the best-fitted calculations of the diffuseness parameters.
6. In $^{16}O+^{63}Cu$, from the comparison of results, we conclude that the higher the surface diffusion parameter value a_0, the smaller the nuclear potential V_0, and vice versa, whether SC or CC, both when $E_{c.m.}$ and r_0 (fm) are fixed.

3.4 Future Work

It is also well recognized that future research is needed to uncover many of the features that influence mathematical computations, thus we provide some recommendations:

1. Investigate the surface diffuseness parameters for another inter-nucleus potential heavy system using quasi-elastic scattering.
2. Investigate the surface diffuseness parameters of the nuclear potential for the system using medium-heavy mass projectiles for the same heavy target.
3. Study the nuclear potential surface diffuseness parameters for the same systems but at sub- barriers energies .
4. Search the difference between the diffuseness parameters that the quasi-elastic scattering was obtained from wide angle and cross-sections of fusion.
5. Measure the difference between the diffuseness measurements derived from wide angle quasi-elastic scattering at deep and sub-barrier energies.

References

References

[1] K. Hagino, T. Takehi, A. B. Balantekin, and N. Takigawa, Phys. Rev. C **71**, 044612 (2005).

[2] K. Washiyama, K. Hagino, and M. Dasgupta, Phys. Rev. C **73**, 034607 (2006).

[3] L. R. Gasques, M. Evers, D. J. Hinde, M. Dasgupta, P. R. S. Gomes, R. M. Anjos, M. L. Brown, M. D. Rodr´ıguez, R. G. Thomas, and K. Hagino, Phys. Rev. C **76**, 024612 (2007).

[4] I. J. Thompson, Comput. Phys. Rep. **7**, 167 (1988).

[5] J. Raynal, Phys. Rev. C **23**, 2571 (1981).

[6] K. Hagino, M. Dasgupta, I. Gontchar, D. Hinde, C. Morton, and J. Newton, "Surface diffuseness anomaly in heavy-ion fusion potentials, In Perspectives In Heavy Ion Physics", World Scientific, pp. 87-98 (2002).

[7] K. Hagino, N. Rowley, and A. Kruppa, Comput. Phys. Commun. **123**, 143 (1999).

[8] K. S. Jassim, F. A. Mageed, and G. S. Jassim, Int.J.Sci.Res **3**, 1514 (2014).

[9] M. L. Inche Ibrahim, M. Zamrun, and H. A. Kassim, Phys. Rev. C **87**, 024611 (2013)

[10] K. Hagino, Tours Symposium on Nucl. Phys. VI **891**, 80 (2007)

[11] K. Hagino and N. Rowley, Phys. Rev. C **69**, 054610 (2004).

[12] M. Zamrun, K. Hagino, S. Mitsuoka, and H. Ikezoe, Phys. Rev. C **77**, 034604 (2008).

[13] G. Kaur, B. Behera, P. Sharma, M. Thakur, and R. Mahajan, Proceedings of the DAE Symp. on Nucl. Phys. **59**, 530 (2014).

[14] M. Beckerman, Phys. Rep. **129**, 145 (1985).

[15] K. Hagino and K. Washiyama, AIP conf. proc. **853** (1), 86-93 (2006).

[16] C. Lin, H. Jia, H. Zhang, F. Yang, X. Xu, F. Jia, Z. Liu, and K. Hagino, Phys. Rev. C **79**, 064603 (2009).

[17] D. Monteiro, J. Shorto, J. Huiza, P. Gomes, and E. Crema, Phys. Rev. C **76**, 027601 (2007).

[18] R. A. Broglia and A. Winther, Heavy Ion Reactions: The Elementary Processes (No. 84). Addison-Wesley Publishing Company, (1991).

[19] P. R. Christensen and A. Winther, Phys. Lett. B **65**, 19 (1976).

[20] M. Lozano and G. Madurga, Nucl. Phys. A **334**, 349 (1980).

[21] L. C. Chamon, D. Pereira, E. S. Rossi, C. P. Silva, H. Dias, L. Losano, and C. A. P. Ceneviva, Nucl. Phys. **A597**, 253 (1996).

[22] M. A. G. Alvarez, L. C. Chamon, D. Pereira, E. S. Rossi, C. P. Silva, L. R. Gasques, H. Dias, and M. O. Roos, Nucl. Phys. A **656**, 187 (1999).

[23] C. P. Silva, M. A. G. Alvarez, L. C. Chamon, D. Pereira, M. N. Rao, E. S. Rossi Jr., L. R. Gasques, M. A. E. Santo, R. M. Anjos, J. Lubian, P. R. S. Gomes, C. Muri, B. V. Carlson, S. Kailas, A. Chatterjee, P. Singh, A. Shrivastava, K. Mahata, S. Santra, Nucl. Phys. A **679** (3-4), 287-303 (2001).

[24] M. M. Evers, "Systematics of near-barrier nuclear reactions using quasi-elastic scattering", Ph.D. thesis, The Australian National University (2010).

[25] M. V. Andres, N. Rowley, and M. A. Nagarajan, Phys. Lett. B **202** (3), 292-295 (1988).

[26] H. Timmers, J. Leigh, M. Dasgupta, D. Hinde, R. Lemmon, J. Mein, C. Morton, J. Newton, and N. Rowley, Nucl. Phys. A **584**, 190 (1995).

[27] C. Morton, A. Berriman, M. Dasgupta, D. Hinde, J. Newton, K. Hagino, and I. Thompson, Phys. Rev. C **60**, 044608 (1999).

[28] S. Sastry and S. Santra, Pram. **54**, 813-826 (2000).

[29] T. J. Schuck, H. Timmers, and M. Dasgupta, Nucl. Phys. A **712**, 14-22 (2002).

[30] I. Gontchar, D. Hinde, M. Dasgupta, and J. Newton, Nucl. Phys. A **722**, C479-C483 (2003).

[31] K. Hagino, AIP conf. proc. **891** (1), 80-88 (2007).

[32] K. Hagino, AIP conf. proc. **1120** (1), 3-8 (2009).

[33] I. Dutt and R. K. Puri, Phys. Rev. C **81**, 047601 (2010).

[34] V. Scuderi, A. Di Pietro, L. Acosta , F. Amorini, M. J. G. Borge, P. Figuera, M. Fisichella, L. M. Fraile, J. Gomez-Camacho, H. Jeppesen, M. Lattuada, I. Martel, M. Milin, A. Musumarra, M. Papa, M.G. Pellegriti, F. Perez-Bernal, R. Raabe, G. Randisi, F. Rizzo, D. Santonocito, G. Scalia, O. Tengblad, D. Torresi, A.M. Vidal, M. Zadro J. of Phys. : Conf. Ser. **381** (1), 012050 (2012).

[35] S. Yusa, K. Hagino, and N. Rowley, Phys. Rev. C **88**, 054621 (2013).

[36] K. S. Jassim, Int. J. of Sc. and Res. **3**, 1514- 1518 (2014).

[37] F. A. Majeed, K. S. Jassim, and N. H. Abbas, IJSR **3**, 315 (2014).

[38] K. Hagino and N. Rowley, EPJ Web of Conf. **86**, 00014 (2015)

[39] V. Kovalchuk, Russ. Phys. J. **58**, 1134-1140 (2015).

[40] J. P. Fernández-García, A. Di Pietro, P. Figuera, M. Fisichella, M. Lattuada, A. M. Moro, A. Musumarra, M. G. Pellegriti1, V. Scuderi1, D. Torresi and M. Zadro, EPJ Web of Conf. **117**, 06012 (2016).

[41] K. S. Jassim, and S. R. Sahib, J. of Chem. and Phar. Sc. **10** (3), 1214 (2017).

[42] T. Tanaka, Y. Narikiyo, K. Morita, K. Fujita, D. Kaji1, K. Morimoto, S. Yamaki1, Y. Wakabayashi, K. Tanaka, M. Takeyama, A. Yoneda, H. Haba1, Y. Komori, S. Yanou, B. Jean-Paul Gall, Z. Asfari, H. Faure, H. Hasebe, M. Huang, J. Kanaya, M. Murakami, A. Yoshida, T.

Yamaguchi, F. Tokanai, T. Yoshida, S. Yamamoto, Y. Yamano, K. Watanabe, S. Ishizawa, M. Asai, R. Aono, S. Goto, K. Katori, and K. Hagino, J. of Phys. Soc. of Jap. **87** (1), 014201 (2018).

[43] Q. J. Tarbool, K. S. Jassim, and A. A. Abojassim, Int. J. of Nucl. En. Sc. and Tech. **13** (2), 110-119 (2019).

[44] A. J. Hassan, and K. S. Jassim, NeuroQuantology, **18** (9), 40 (2020).

[45] L. F. Canto, P. R. S. Gomes, R. Donangelo, and M. S. Hussein, Phys. Rep. **424**, 1 (2006).

[46] J. K. Tuli, A Manual for Preparation of Data Sets-National Nuclear Data Center Brookhaven National Laboratory PO Box, **5000**, 11973-5000 (2001).

[47] I. J. Thompson and M. A. Nagarajan, Phys. Lett. B **106**, 163 (1981).

[48] N. Rowley,G.R. Satchler, and P.H. Stelson, Phys. Lett. B **254**, 25 (1991).

[49] M. Dasgupta, D. J. Hinde, N. Rowley, and A. M. Stefanini, Annu. Rev. Nucl. Part. Sci. **48**, 401 (1998).

[50] N. Rowley, H. Timmers, J. R. Leigh, M. Dasgupta, D. J. Hinde, J. C. Mein, C. R. Morton, and J. O. Newton, Phys. Lett. B **373**, 23 (1996).

[51] M. L. Inche Ibrahim, "Analysis of the nuclear potential for heavy-ion systems through large-angle quasi-elastic scattering", Ph.D. Thesis, Doctoral dissertation, University of Malaya (2012).

[52] K. Hagino and N. Takigawa, Pr. of Th. Phys. **128**,1061-1106 (2012).

[53] M. Dasgupta, D. Hinde, J. Newton, and K. Hagino, Prog. Theo. Phys. Suppl. **154**, 209 (2004).

[54] M. Ismail, W. Seif, H. Abou-Shady, and A. Bakry, Phys. of Atom. Nucl. **69**, 1463-1471 (2006).

[55] R. A. Broglia and A. Winther, "Heavy Ion Reactions: Elastic and inelastic reactions" vol. 52: Benjamin-Cummings Publishing Company (1981).

[56] T. E. O. Ericson, Ann. Phys. **281**, 494-518 (2000).

[57] Y. B. Band, K. F. Freed, and D. J. Kouri, J. of Chem. Phys. **74**, 4380-4394 (1981).

[58] S. Landowne and S. C. Pieper, Phys. Rev. C **29**, 1352 (1984).

[59] M. Y. Kuchiev and V. Flambaum, Phys. Rev. D **70**, 044022 (2004).

[60] S. Yusa, K. Hagino, and N. Rowley, Phys. Rev. C **85**, 054601 (2012).

[61] A. Balantekin and N. Takigawa, Rev. of Mod. Phys. **70**, 77 (1998).

[62] A. Berriman, D. Hinde, M. Dasgupta, C. Morton, R. Butt, and J. Newton, Nat. **413**, 144-147 (2001).

[63] J. Hietarinta, B. Grammaticos, B. Dorizzi, and A. Ramani, Phys. Rev. lett. **53**, 1707 (1984).

[64] S. K. Gray and D. E. Manolopoulos, J. of Chem. Phys. **104**, 7099-7112 (1996).

[65] R. E. Olson, F. Smith, and E. Bauer, Appl. Opt. **10**, 1848-1855 (1971).

[66] H. Rose and D. Brink, Rev. of Mod. Phys. **39**, 306 (1967).

[67] M. Giles, "Non-reflecting boundary conditions for the Euler equations: Computational Fluid Dynamics Laboratory" Department of Aeronautics and Astronautics, Massachusetts Institute of Technology, (1988).

[68] M. Moshinsky, J. of Phys. A **26**, 2445 (1993).

[69] H. S. Bosch and G. Hale, Nucl. Fus. **32**, 611 (1992).

[70] H. Esbensen, S. Landowne, and C. Price, Phys. Rev. C **36**, 1216 (1987).

[71] K. McLenithan and D. Secrest, J. of Chem. Phys. **80**, 2480-2503 (1984).

[72] M. N. I. Naala, "Moderating and mediating roles of human capital and competitive advantage on entrepreneurial orientation, social network

and performance of SMEs in Nigeria" University Utara Malaysia, (2016).

[73] K. Hagino, N. Takigawa, A. Balantekin, and J. Bennett, Phys. Rev. C **52**, 286 (1995).

[74] A. Kruppa, P. Romain, M. Nagarajan, and N. Rowley, Nucl. Phys. A, **560**, 845-862 (1993).

[75] A. Balantekin, A. DeWeerd, and S. Kuyucak, Phys. Rev. C **54**, 1853 (1996).

[76] E. Huttel, W. Arnold, H. Baumgart, and G. Clausnitzer, Nucl. Inst. and Meth. in Phys. Res. B **12**, 193-199 (1985).

[77] A. Bohr, "Mottelson. Nuclear Structure", Benjamin, New York, (1975).

[78] M. Dasgupta, D. Hinde, A. Mukherjee, and J. Newton, Nucl. Phys. **A 787**, 144-149 (2007).

[79] A. Trzcińska, E. Piasecki, K. Hagino, W. Czarnacki, P. Decowski, N. Keeley, M. Kisielinski, P. Koczon, A. Kordyasz, E. Koshchiy, M. Kowalczyk, B. Lommel, A. Stolarz, I. Strojek, and K. Zerva, Phys. Rev. C **92**, 034619 (2015).

[80] A. B. B. Mottelson, "Nuclear Structure", WA Benjamin Inc., New York, Amsterdam (1975).

[81] R. White, M. Sparks, and I. Ortenburger, Phys. Rev. **139**, A450 (1965).

[82] N. S. Brady, "Relativistic Coulomb Excitation of the Pygmy Dipole and Giant Resonances" Texas A and M University Commerce (2016).

[83] J. Cipriani and B. Silvi, Mol. Phys. **45**, 259-272 (1982).

[84] S. Goldman, Phys. Rev. A **31**, 3541 (1985).

[85] W. A. Benalcazar, B. A. Bernevig, and T. L. Hughes, Sc. **357**, 61-66 (2017).

[86] S. Polarz and B. Smarsly, J. of nan. and nan. **2**, 581-612 (2002).

[87] R. Naik, "Studying fusion reactions for effect of PCN on heavy nucleus formation and for nuclear structure effects" Ph.D. thesis, Oregon State University (2007).

[88] J. O. Newton, R. D. Butt, M. Dasgupta, D. J. Hinde, I. I. Gontchar, and C. R. Morton, Phys. Rev. C **70**, 024605 (2004).

[89] S. Raman, C. Nestor, and P. Tikkanen, Atom. Data and Nucl. Data Tabl. **78**, 1-128 (2001).

[90] M. Zadro, P. Figuera, A. Di Pietro, M. Fisichella, M. Lattuada, T. L¨onnroth, M. Milin, V. Ostashko, M. G. Pellegriti, V. Scuderi, D. Stanko, E. Strano, and D. Torresi, Phys. Rev. C, **87** (5), 054606 (2013).

[91] H. Leucker, K. Becker, K. Blatt, W. Korsch, W. Luck, H. Reich, H. G. Volk, D. Fick R. Butsch, H.-J. Jansch, and Z. Moroz, Phys. Rev. lett. **62** (19), 2241 (1989).

[92] Y. Y. Yang, J. S. Wang, Q. Wang, D. Y. Pang, J. B. Ma, M. R. Huang, P. Ma, S. L. Jin, J. L. Han, Z. Bai, L. Jin, J. B. Chen, Q. Hu, R. Wada, S. Mukherjee, Z. Y. Sun, R. F. Chen, X. Y. Zhang, Z. G. Hu, X. H. Yuan, S. W. Xu, S. Z. Chen,X. G. Lei, L. X. Liu, W. H. Ma, S. T. Wang, D. Yan, X. H. Zhang, M. H. ZhaoY. Zhou,Y. J. Zhou, Z. Y. Guo, Y. H. Zhang, H. S. Xu, and G. Q. Xiao, Phys. Rev. C **90** (1), 014606 (2014).

[93] N. Wang, and W. Scheid, Phys. Rev. C, **78** (1), 014607 (2008).

الخلاصة

في هذه الدراسة تم اجراء دراسة منهجية عن الاستطارة شبه المرنة تم من خلالها قياس تأثير معامل الانتشار السطحي للجهد النووي على حسابات المقطع العرضي للاستطارة شبه المرنة الى المقطع العرضي لاستطارة رذرفورد وقد تم اخذها في جميع مراتب الاقتران القناة المنفردة (SC) والقنوات المزدوجة (CC). هذه الاستطارة شبه المرنة تحدث بين نواتين ولاكثر من منظومة. المنظومات المستخدمة في الدراسة الحالية هي : $^{6}Li+^{64}Zn,^{23}Na+^{90}Zr,^{11}C+^{208}Pb,^{16}O+^{208}Pb,^{63}Cu+^{208}Pb$. الجهد الذي يصف التفاعلات بين النوى يتالف من جهد كولوم والجهد النووي . الجهد النووي تم وصفه باستخدام نمط وود – ساكسون(WS) . تم تنفيذ حسابات القناة المنفردة(SC) والقنوات المزدوجة (CC) التي تصف الحركة النسبية للنوى المتصادمة وحركاتها الذاتية لدراسة تاثيرها على حسابات نسبة المقطع العرضي للاستطارة شبه المرنة الى المقطع العرضي لاستطارة رذرفورد، وقد تم التحقيق للعثور على افضل قيمة ملائمة لمعلمات الانتشار مقارنة بالبيانات التجريبية.

البرنامج المستخدم في هذه الدراسة CQEL والذي طور من قبل الباحث الياباني هاكينو وزملائه. استخدمنا طريقة مربع كاي χ^2 لايجاد افضل تطابق لقيمة معلمة الانتشار مع البيانات التجريبية. افضل معلمة انتشار تم الحصول عليها من خلال حسابات قناة الاقتران لقذيفة خاملة وهدف متهيج هي للانظمة $^{6}Li+^{64}Zn,^{23}Na+^{90}Zr,^{11}C+^{208}Pb,^{16}O+^{208}Pb$ ومن هدف خامل وقذيفة متهيجة هي للنظام $^{63}Cu+^{208}Pb$. ان معلمات الانتشار التي تم الحصول عليها مقارنة مع القيمة القياسية البالغة $a_0 = 0.63$ fm فهي متوافقة تماما مع جميع الانظمة المذكورة اعلاه .

جمهورية العراق
وزارة التعليم العـــالي والبحث العلـمي
جامـــعة بابـــل
كليـــة التربية للعلوم الصرفة
قســـم الفيزيـــاء

دراسة تحليلية للاستطارة شبه المرنة لبعض الانظمة باستخدام جهد وود-ساكسون

رسالة مقدمة

إلى مجلس كلية التربية للعلوم الصرفة في جامعة بابل

وهي جزء من متطلبات نيل درجة الماجستير

في التربية / الفيزياء

من قبل الطالبة

نغم حسن حايف علي

بكالوريوس تربية فيزياء

(2003)

بأشراف

أ.د. خالد صالح جاسم

1443 هـ

2021 م